Journal of Medicinal Chemistry

Article

Studies on aryl-substituted phenylalanines - synthesis, activity and different binding modes at AMPA receptors

Ewa Szymanska, Karla Frydenvang, Darryl S Pickering, Christian Krintel, Birgitte Nielsen, Ayesheh Kooshki, Linda G. Zachariassen, Lars Olsen, Jette Sandholm Kastrup, and Tommy N. Johansen

J. Med. Chem., **Just Accepted Manuscript** • DOI: 10.1021/acs.jmedchem.5b01666 • Publication Date (Web): 12 Dec 2015

Studies on aryl-substituted phenylalanines - synthesis, activity and different binding modes at AMPA receptors

Ewa Szymanska,[a,b,c] Karla Frydenvang,[a,c] Darryl S. Pickering,[a] Christian Krintel,[a] Birgitte Nielsen,[a] Ayesheh Kooshki,[a] Linda G. Zachariassen,[a] Lars Olsen,[a] Jette S. Kastrup,[a] and Tommy N. Johansen[a*]*

[a]Department of Drug Design and Pharmacology, Faculty of Health and Medical Sciences, University of Copenhagen, 2100 Copenhagen Ø, Denmark; [b]present affiliation: Department of Technology and Biotechnology of Drugs, Jagiellonian University Medical College, Medyczna 9, PL 30-688 Kraków, Poland.

Keywords

ionotropic glutamate receptors, GluA2, competitive antagonist, chiral resolution, X-ray structure, molecular modeling

Abstract

A series of racemic aryl-substituted phenylalanines was synthesized and evaluated *in vitro* at recombinant rat GluA1–3, at GluK1–3 and at native AMPA receptors. The individual enantiomers of two target compounds, (*RS*)-2-amino-3-(3,4-dichloro-5-(5-hydroxypyridin-3-yl)phenyl)propanoic acid **37** and (*RS*)-2-amino-3-(3'-hydroxybiphenyl-3-yl)propanoic acid **38** were characterized. (*S*)-**37** and (*R*)-**38** were identified as the only biologically active isomers, both being antagonists at GluA2 receptors with K_b of 1.80 and 3.90 μM, respectively. To address this difference in enantiopharmacology, not previously seen for amino acid-based AMPA receptor antagonists, X-ray crystal structures of both eutomers in complex with the GluA2 ligand binding domain were solved. The co-crystal structures of (*S*)-**37** and (*R*)-**38** showed similar interactions of the amino acid parts, but unexpected and different orientations and interactions of the bi-aromatic parts of the ligands inside the binding site, with (*R*)-**38** having a binding mode not previously identified for amino acid-based antagonists.

Introduction

Most excitatory neurotransmission within the mammalian central nervous system is mediated by the ionotropic glutamate receptors (iGluRs), which include three functionally distinct subclasses named according to their selective affinity for the specific agonists: *N*-methyl-D-aspartic acid (NMDA), (*RS*)-2-amino-3-(3-hydroxy-5-methyl-4-isoxazolyl)propionic acid (AMPA) and kainate (KA).[1, 2] All three subclasses of iGluRs play an important role in controlling synaptic plasticity, underlying learning and memory processes. On the other hand, the excessive activation of calcium-permeable NMDA receptors (and in some circumstances AMPA receptors) leads to abnormal Ca^{2+} influx that can initiate neurotoxic intracellular signaling cascades and neuronal cell death observed in several neurological diseases, including stroke, Alzheimer, Parkinson, Huntington and neuropathic pain.[3, 4]

Structurally, iGluRs are tetrameric assemblies of subunits encoded by separate genes. Native AMPA and kainate receptors are homo- or heterooligomers formed by subunits GluA1–GluA4 and GluK1–GluK5, respectively. In case of the NMDA subclass seven subunits denoted GluN1, GluN2A–GluN2D and GluN3A–GluN3B have been cloned and characterized.[1] Each individual subunit consists of an extracellular amino-terminal domain (ATD), an extracellular ligand binding domain (LBD), a transmembrane domain that forms the cation-selective pore and a cytoplasmatic C-terminal domain involved in receptor localization and modulation.

Taking into account the role of iGluRs in a variety of neurological disorders, the development of subtype-specific competitive antagonists as neuroprotective agents is of considerable therapeutic interest. Over the past decades a wide group of competitive antagonists of non-NMDA iGluRs has been developed, however, due to a highly conserved nature of the LBD only few of them show subtype selectivity.[2, 5-7] Structurally, most of the known competitive antagonists belong to one of two major classes: 1) expanded versions of agonists and 2) quinoxalines (Figure 1).[2] The first class includes compounds with an α-amino acid motif of agonists and a distal negatively charged group, most often a carboxylate, phosphonate or tetrazolyl ring. Typical representatives of this category are isoxazole-based compounds[8, 9] [*e.g.* (*S*)-ATPO (**1**)], willardiine derivatives[10] (*e.g.* UBP310 (**2**)) or

cis-decahydroisoquinolines[11, 12] (*e.g.* tezampanel (**3**)). Furthermore, it has been shown that a series of phenylalanine derivatives (such as compound **4**) also belong to this class.[13, 14] The second class of non-NMDA iGluRs competitive antagonists comprises a variety of quinoxalines,[15, 16] represented by NBQX (**5**) or ZK-200775 (**6**). Some structurally dissimilar competitive AMPA receptor antagonists, such as the isatine oxime NS1209 (**7**), have also been described.[17, 18]

The advances in crystallography of soluble constructs of LBDs of iGluRs in complex with agonists and competitive antagonists have provided information on receptor motifs for recognition of structurally diverse ligands.[10, 19-21] Comparison of crystal structures of the GluA2 or GluK1 subtype LBD with bound α-amino acid-based compounds reveals the preserved binding mode of the α-amino acid fragment for both agonists and competitive antagonists, while the distal fragment of antagonist structures interacts with residues of domain D2 with a foot-in-the-door mechanism, stabilizing the open conformation of the receptor. Furthermore, a predominant amount of these compounds bind with their α-amino acid part in the *S*-configuration,[20] although few examples of *R*-configured amino acid-based ligands are known.[22-25]

In a previous study, we have reported a new series of phenylalanines with a rigid or a flexible biaromatic ring system (Figure 2A).[26] Among these compounds, the dichloro-substituted biphenyl analogue substituted with a hydroxyl group in position 3 of the distal phenyl ring (**9**) showed selective affinity to AMPA receptors (IC_{50} = 4.6 μM), while the similar compound with a 3-carboxylic substituent turned out to bind selectively to GluK1 receptors (K_i = 2.8 μM). Encouraged by these results we report here the synthesis and chiral chromatography resolution of a new series of aryl substituted phenylalanines (Figure 2B) as well as their biological evaluation at native and selected recombinant homomeric iGluRs. Furthermore, crystal structures were solved of selected eutomers bound to the LBD of the GluA2 subunit to investigate the binding modes at AMPA receptors.

Results

In the series of the target amino acids we kept the biaryl core of compounds with an additional phenyl or pyridine ring introduced into the 5-position of the phenylalanine ring (Figure 2B). The structural modifications were focused mainly on the distal ring, namely: 1) a change of the position and the number of hydroxyl groups, 2) replacement of the hydroxyl substituent of (**9**) and (**10**) with either an amino or sulfonamide group, 3) blockade of the hydrogen donor availability of the hydroxyl group by introducing an alkyl fragment. Taking into account the influence of the presence of two chlorines on AMPA receptor affinity,[26] in most of new compounds we preserved the dichlorophenylalanine substitution pattern.

Chemistry

The synthesis of new amino acids was based on previously developed convergent synthesis strategies[26] (Schemes 1 and 2). Treatment of 3-iodotoluene precursors **11** and **12** with NBS under free radical conditions, followed by substitution with the sodium salt of diethyl acetamidomalonate afforded the key intermediates **13** and **14**. The final amino acids **27**-**38** were prepared as a result of a number of Suzuki coupling reactions of aryl iodides **13** and **14** with boronic acids or esters, followed by deprotection in 48% aqueous hydrobromic acid (or, in case of **30** and **31**, in aqueous hydrochloric acid and acetic acid) and purified by reverse-phase HPLC.

Synthesis of *S*- and *R*-enantiomers of **38** was performed in a similar way (Scheme 2). Ethyl esters of commercially available (*S*)- and (*R*)-*N*-Boc-3-bromophenylalanine were reacted with 3-methoxyphenylboronic acid under Suzuki conditions. Deprotection and purification by reverse-phase HPLC gave the desired amino acids (*S*)-**38** (ee = 98.3%) and (*R*)-**38** (ee = 98.0%).

Chromatographic resolution of racemic **37** was carried out by chiral HPLC using the Chirobiotic T column.[27, 28] The first-eluting (+)-isomer as well as the late-eluting (−)-isomer were isolated in good to high stereochemical purity (ee > 97% and 99.7%, respectively). In order to address the configurational assignment of (+)- and (−)-**37**, the elution order of (+)- and (−)-**37** as well as (*R*)-(−)-

and (*S*)-(+)-**38** were studied using the Chirobiotic T column and using a ligand-exchange HPLC column which contains (*R*)-Pro as a chiral selector.[29] As expected for α-amino acids,[28, 29] (*S*)-(+)-**38** is the first eluting enantiomer both on the Chirobiotic T and on the (*R*)-Pro columns. When analyzed on the (*R*)-Pro column, (+)-**37** turned out to be the first eluting enantiomer. Thus, the elution order of (+)- and (−)-**37** on two columns with different chiral selectors indicate that (+)-**37** has *S*-configuration. The configurational assignment of (*S*)-(+)-**37** was later supported by X-ray crystallography (See Structure Determination for further details).

Binding Pharmacology

The results of *in vitro* pharmacological activity at native AMPA receptors in rat cortical membranes for compounds **27**–**38** (and, for comparison, for previously described **8**–**10**[26]) are given in Table 1. Among the tested dichlorosubstituted phenylalanines, only amino acids possessing a 3-hydroxyl substituent in the distal aromatic ring showed measurable affinity to AMPA receptors (**27**, **28**, **37**, **38**), with IC_{50} values in the range of 1.5–16 μM. The introduction of an additional hydroxyl group into the distal phenyl did not enhance binding at AMPA receptors; however, a 2–3-fold decrease in affinity for **27** and **28** was observed relative to the reference compound **9**. The exchange of the hydroxyl for an ether group (**29**, **30**), a sulfonamide (**34**, **35**) or even a hydroxymethyl group (**31**, **32**) significantly decreased or completely removed the affinity. No affinity (IC_{50} > 100 μM) was observed for **33**, in which the hydroxyl group in the 3-position was replaced with an amino group.

Modification of the distal aryl and exchange of a phenyl for a pyridine ring, keeping the hydroxyl substitution pattern of **9**, yielded the most potent AMPA receptor ligand, (*RS*)-2-amino-3-(3,4-dichloro-5-(5-hydroxypyridin-3-yl)phenyl)propanoic acid (**37**) with affinity determined to 1.5 μM, whereas the regional isomer **36** showed no AMPA receptor affinity (IC_{50} > 100 μM). Furthermore, compound **38**, which was included within the present series as a close structural analogue of **9** without the dichloro pattern in the phenylalanine ring, showed an AMPA receptor affinity comparable with that of **9**. In AMPA receptor binding studies using enantiomerically pure **37** and **38,**

(*S*)-**37** and (*R*)-**38** were clearly identified as the respective eutomers (Table 1). In the homogenate binding studies to native KA and NMDA receptors as well as binding studies to recombinant rat GluK1 homomeric kainate receptors expressed in *Sf9* insect cell membranes, all target compounds showed either very weak micromolar (50 – 100 μM) or no affinity (> 100 μM).

The individual enantiomers of the two most active compounds among the present series of phenylalanines, **37** and **38**, were subsequently characterized at the cloned rat GluA1–3 and GluK1–3 receptors (Table 2). In these radioligand binding assays the *S*-enantiomer of **37** also was found to be responsible for the biological activity of the racemic compound at GluA1–3 homomeric receptors with the strongest binding to the GluA2 receptor (K_i = 1.7 μM), and at the same time showing no affinity (K_i > 100 μM) to any of the homomeric GluK1–3 receptors. A 4-fold higher affinity at GluA2 relative to GluA1 and GluA3 ($P < 0.0001$, one-way ANOVA with Holm-Sidak post-test) was observed for this compound; however, no statistically significant difference was found between affinity to GluA1 and GluA3 receptors. The *R*-enantiomer of **37** was inactive at all tested recombinant receptors (K_i > 100 μM).

In contrast to **37** and most other α-amino acid-based ligands of AMPA receptors, but in agreement with the stereoselectivity observed in AMPA receptor binding to native receptors (Table 1), only the *R*-enantiomer of **38** was found to show biological activity, while (*S*)-**38** lacked affinity to both homomeric AMPA and kainate receptors (K_i > 100 μM; Table 2). (*R*)-**38** presented micromolar binding to both recombinant GluA1-3 receptors as well as to kainate recombinant GluK3 receptors (Table 2).

Functional Pharmacology

Using two electrode voltage clamp (TEVC) electrophysiology the antagonist properties of (*S*)-**37** and (*R*)-**38** were examined at homomeric GluA2(Q)$_i$ receptors expressed in *X. laevis* oocytes. As shown in Figure 3, (*S*)-**37** dose-dependently antagonized the responses to (*S*)-Glu. The functional K_b value of (*S*)-**37** at GluA2(Q)$_i$ was determined to be 1.80 μM, which is not statistically significantly

different from its respective K_i value (1.74 μM) determined from radioligand binding experiments at full length GluA2(R)$_o$ (P = 0.949, t-test) (Table 2). (R)-**38** antagonized (S)-Glu responses with a calculated K_b value of 3.90 μM, which was more potent than the observed GluA2(R)$_o$ binding affinity (K_i = 24 μM). Application of either 0.60 mM (S)-**37** or 1 mM (R)-**38**, in the presence of 100 μM cyclothiazide, did not produce any detectable agonist responses at GluA2(Q)$_i$, indicating that neither (S)-**37** nor (R)-**38** show partial agonist effects at these concentrations under our experimental conditions. However, it cannot be completely ruled out that partial agonism may be seen at much higher concentrations of the compounds.

Structure determination

The GluA2 LBD (GluR2-S1S2J) was co-crystallized with (S)-**37** and (R)-**38**, respectively, and formed GluA2 dimeric complexes in both cases. In the co-crystal structures (S)-**37** as well as (R)-**38** were located in the (S)-Glu binding cleft of the LBD, but found to adopt very different binding modes.

The structure of GluA2 LBD with (*S*)-37. The structure of GluA2 LBD in complex with (S)-**37** was solved at 2.0 Å resolution, and the complex crystallized in space group $P2_12_12$ with one molecule in the asymmetric unit of the crystal. A two-fold symmetrical dimer of GluA2 LBD is formed by interaction with a symmetry-related molecule as previously seen.[19] For further information on data collection and refinement statistics, see Table 3. (S)-**37** induces partial LBD domain opening (rigid body movements of lobes D1 and D2) of 13.5° of the GluA2 LBD, relative to the structure with Glu (PDB ID 1FTJ, molB[19]) (Figure 4A). The Ile633-Ile633(sym) linker-linker distance of 32.6 Å is intermediate among the linker-linker distances observed for full agonists and antagonists, in accordance with the partial domain opening.[20]

Generally, the electron density is well defined and (S)-**37** could unambiguously be modelled into the density (Figure 4B), thus confirming the absolute configuration indicated by the chiral HPLC analyses. The binding mode of (S)-**37** at GluA2 LBD resembles that of other amino acid-based

competitive antagonists.[9, 10, 13, 23] Compared to these antagonists, the α-carboxyl and α-amino groups of (*S*)-**37** are observed at the same position in the GluA2 binding cleft and show the same type of hydrogen bonding interactions to surrounding residues (Pro478, Thr480, Arg485 and Glu705; full length numbering without signal peptide).

The hydroxy-pyridine moiety of (*S*)-**37** is accommodated in a cavity formed by the residues Thr649, Leu650, Thr655, Thr686, Tyr702, Leu703, Leu704 and Glu705 (Figure 4C). Two hydrogen bonds are formed between the hydroxyl group of (*S*)-**37** and the side-chain hydroxyl groups of Thr686 and Tyr702, as well as one hydrogen bond between the pyridine N-atom of (*S*)-**37** and the side chain hydroxyl group of Thr655 (Figure 4B). The aromatic ring with the two chlorine atoms is located in an area close to residues Glu402, Tyr405, Pro478, Met708 and Tyr732 (Figure 4B). The residue Met708 is found in a conformation with the side chain pointing away from the binding cleft to avoid steric repulsion. The presence of the two aromatic rings prohibits the interlobe hydrogen bond seen in structures with agonists,[19] between residues Glu402 in D1 and Thr686 in D2 (distance is 4.5 Å). A molecule of glycerol is found in this area where it is involved in a hydrogen-bond bridge between these two residues (Figure 4C).

The structure of GluA2 LBD with (*R*)-38. The structure of GluA2 LBD in complex with (*R*)-**38** was solved at 1.8 Å resolution, and the complex crystallized in space group $P2_12_12_1$ with four molecules in the asymmetric unit of the crystal. In this structure, two non-crystallographic two-fold dimers are formed (molA/molC and molB/molD, respectively). For further information on data collection and refinement statistics, see Table 3. (*R*)-**38** induces full domain opening (20.2°, 20.4°, 19.2° and 18.8° for molA, molB, molC and molD, respectively) of the GluA2 LBD, relative to the structure with Glu (PDB ID 1FTJ, molB[19]) (Figure 4D). The domain opening is similar to the opening of the apo structure of GluA2 LBD (molA, 21.1°, PDB ID 1FTO[19]). The linker-linker distances are 26.9 Å (dimer A/C) and 26.7 Å (dimer B/D) in accordance with full domain opening.[20] Generally, the electron density is well defined and (*R*)-**38** could unambiguously be modelled into the density (Figure 4E). The amino-acid part of (*R*)-**38** forms contacts to binding-site residues in a

comparable manner to that of (*S*)-**37** (Figures 4E and 4B). The bi-cyclic aromatic system of (*R*)-**38** is accommodated in a new cavity close to the hinge region formed by the residues Thr480, Thr482, Leu498, Ile500, Ser654, Glu705, Asp728 and Lys730 (Figure 4F). The hydroxyl group of (*R*)-**38** makes two hydrogen bonds; one to the side chain carboxylate of Asp728 and one to a water molecule. The presence of the two aromatic rings in the hinge region prevents domain closure by steric hindrance and thereby the formation of a hydrogen bond between Glu402 in D1 and Thr686 in D2 (distance is 6.5 Å).

Molecular docking studies

In order to analyze the observed structure-activity relationship SiteMaps of ligand binding sites were generated and docking studies carried out. The SiteMaps show that the amino acid parts of (*S*)-**37** and (*R*)-**38** fits well into the acceptor and donor regions (Figure 5). The chlorine atom in the 5-position of the phenylalanine ring fits into a hydrophobic region. Moreover, there are small acceptor and donor regions close to the hydroxy-pyridinyl part of (*S*)-**37**, representing hydrogen bonds between Thr655, Thr686 and Tyr702 and the heteroatoms of the hydroxy-pyridinyl group. These small acceptor and donor regions might explain why (*S*)-**37** fits well into this pocket. In the SiteMap of the ligand binding site of (*R*)-**38**, it is of notice that the phenoxy group of (*R*)-**38** fits into a hydrophobic region with no acceptor surface (Figure 5), indicating that (*R*)-**37** would lack an interaction with a hydrogen bonding donor for the hydroxy-pyridinyl nitrogen atom.

Next, all compounds listed in Table 1 were docked into the GluA2 LBD in complex with (*S*)-**37** as their *S*-enantiomer (Table 4). Generally, compounds with measurable affinity have XP-scores that are better than −9 kcal/mol. The inactive analogues **30**, **34** and **35**, with IC_{50} > 100 μM, show only limited XP-scoring in docking experiments, most likely reflecting steric hindrance due to large substituents (Table 1). The inactive 3-methoxy-substituted analogue **29**, having only hydrogen bond acceptor possibilities, shows medium XP-scores but high strain. The two hydroxymethyl substituted analogues **31** and **32** are both inactive and display a relatively good score (–9.3 kcal/mol) and a very

poor XP-score (–1.3 kcal/mol), respectively. Considering the position of the hydroxyl group of **31** compared to **37**, this compound will only be able to form one hydrogen bond since it is positioned too far away from Tyr702. In addition, in order for the hydroxymethyl substituent to interact favorably with Thr655 and/or Tyr702, the 5-chloro substituent of **31** might need to be positioned less favorably as compared to that of compound **37**. Whereas the 3-amino substituted analogue **33** in principle should be able to interact with Thr655 and/or Tyr702 in a manner similar to that of compound **37**, differences in proteolytic properties of the amino-phenyl substituent compared to that of the hydroxypyridyl substituent might explain the inactivity of compound **33**. The inactive pyridyl-substituted analogue **36** seems to be able to form hydrogen bonding interactions with Thr655 but only weak contacts to the side chain of Thr649 as the hydroxyl group of Thr649 already donates a hydrogen bond to the backbone of Leu703. Finally, the two di-hydroxyl substituted analogues **27** and **28** were the best scoring compounds analyzed but showed no improved affinity compared to lead compound **9**. As indicated by the calculated strain energy (Table 4), this might be explained by a strained hydrogen bonding geometry of the hydroxyl groups.

Discussion

In an effort to obtain competitive AMPA receptor antagonists capable of differentiating between the individual AMPA receptor subtypes, we have synthesized a series of α-amino acid-based antagonists. As expected from previously published α-amino acid-based antagonists,[20] the biologically active enantiomer of **37** was found to be in the *S*-configuration, but in the case of the structurally similar analogue **38**, the antagonist activity exclusively was in the *R*-enantiomer. To address this difference in enantiopharmacology we determined the X-ray crystal structures of GluA2 LBD in complex with antagonists (*S*)-**37** and (*R*)-**38**, respectively.

During recent years, a number of ligands have been co-crystallized with the LBD of different iGluRs, revealing that α-amino acid-based ligands adopt similar binding mode of the α-amino acid moiety for both agonists and competitive antagonists. A predominant number of these compounds

bind with their α-amino acid part in the *S*-configuration,[20] although a few examples of *R*-configured amino acid-based ligands have been described, *e.g.* the agonists TDPA[22] and 5-HPCA[24] as well as the antagonists kaitocephalin[23] and IKM-159.[25]

Whereas (*S*)-**37** binds in the expected manner with the aromatic part positioned in an area of the GluA2 binding site often occupied by competitive antagonists (Figure 6A), (*R*)-**38** was found to adopt a new binding mode, in which the aromatic part of the ligand reaches into a cavity not previously occupied by antagonists (Figure 6A). Interestingly, only two structural differences between **37** and **38** (two hydrogen atoms in the phenylalanine ring of **38** instead of the dichloro substitution in **37** as well as a change of a pyridine ring in **37** to phenyl in **38**; Figure 2) led to the opposite stereochemistry of the biologically active enantiomer and very different binding modes. The pyridine nitrogen of **37** allows (*S*)-**37** to form a hydrogen bond to the side-chain hydroxyl group of Thr655, whereas (*S*)-**38** lacks the possibility to form this polar interaction. This might partly explain why (*S*)-**37** shows better affinity than (*S*)-**38** in the (*S*)-**37** binding mode. In addition, the phenyl substituent of (*S*)-**38** would not fit as well into a region of more polar character (Figure 5). On the other hand, in the (*R*)-**38** binding mode the two phenyl rings of (*R*)-**38** fit well into the hydrophobic region, whereas the pyridine ring of (*R*)-**37** would loose a hydrogen bond. The other difference between **37** and **38** is the presence of chlorine atoms in the phenylalanine ring (Figure 2). The chlorine atom of (*S*)-**37** in the 4-position of the phenylalanine ring forces the hydroxy-pyridinyl substituent out-of-the-plane, which has a marked influence on the orientation of the hydroxyl group. Based on the X-ray structures it seems that this out-of-the-plane twist is favorable for optimal hydrogen bonding of the hydroxy-pyridinyl substituent of (*S*)-**37**. However, in the (*R*)-**38** binding mode, it seems likely that a corresponding out-of-the-plane twist may force the hydroxy-aromatic part of the target compound to come too close to the receptor backbone or place the key aromatic hydroxy-substituent in an unfavorable position for interaction with Asp728. Moreover, the chlorine atom in the 5-position of (*S*)-**37** is involved in several favorable contacts to the non-polar part of the (*S*)-**37** binding site (Figure 5). The proteolytic properties of the phenolic hydroxyl groups may also

contribute to the observed pharmacology of **37** and **38**. Since the pK_a-value of the hydroxyl group of 3-hydroxypyridine is lower than that of phenol,[30] the pK_a-value of the hydroxyl group of **37** is likewise lower than that of **38**, with the two electron-withdrawing chlorine atoms of **37** lowering the pK_a even more. Thus, **37** would be stabilized in the (*S*)-**37** binding mode by hydrogen bonding formation to the hydroxyl groups of Thr686 and Tyr702, whereas the interaction from (*R*)-**37** to Asp728 in the (*R*)-**38** binding mode would be repulsive.

Design of subtype selective ligands has been pursued for decades, but despite that a large number of AMPA receptor ligands have been synthesized and characterized pharmacologically, only few of them have shown high AMPA receptor subunit selectivity. Previously, it has been discussed that selectivity of agonists at AMPA receptors might be achieved through interaction of the agonist with the side-chain hydroxyl group of Tyr702 in GluA2 (Tyr698 in GluA1) directly or through water molecules.[31, 32] In GluA3 and GluA4 this residue is Phe, which cannot form side-chain hydrogen bonds. However, for antagonists the same trend has not been observed. The previously described phenylalanine-based antagonist, (*S*)-2-amino-3-(2-(2-carboxyethyl)-5-chloro-4-nitrophenyl)propionic acid, forms a water-mediated contact to Tyr702 but the compound was not selective on AMPA receptor subunits.[13] The present antagonist (*S*)-**37** interacts directly with Tyr702, but again no subunit selectivity is observed for this compound (Table 2). Thus, whereas Tyr702 has been shown to be important for agonist selectivity, it seems to be of minor importance in gaining subunit selectivity of antagonists.

One of the most surprising observed differences between the two resolved crystal structures is the degree of domain opening. Whereas (*R*)-**38** leads to full domain opening (18.8-20.4°), the structure of GluA2 LBD with (*S*)-**37** shows the smallest antagonist induced domain opening of the GluA2 LBD (13.5°) seen to date. As (*S*)-**37** is a functional antagonist, it suggests that compounds may switch from partial agonists to antagonists when domain openings are in the range 11-13°.

Conclusion

In an effort to obtain competitive AMPA receptor antagonists capable of differentiating between the individual AMPA receptor subtypes and to study the relationship between structure and function at the molecular level, we have presented a new series of aryl-substituted phenylalanines, and among these identified two compounds with opposite stereochemistry, (*S*)-**37** and (*R*)-**38**, as eutomers and selective AMPA receptor antagonists with K_b of 1.80 μM and 3.90 μM at recombinant GluA2 AMPA receptors, respectively. Co-crystallization of the two compounds with the GluA2 LBD, followed by X-ray structure determination, revealed that (*S*)-**37** and (*R*)-**38** interact with GluA2 LBD in quite different modes. (*R*)-**38** interacts with the receptor in a new binding mode with the two aromatic rings positioned close to the D1-D2 hinge region. The new binding mode for amino acid based antagonists might be a starting point for the future design of subtype-selective AMPA receptor antagonists. Whereas (*S*)-**37** binds in a conventional manner in GluA2 LBD compared to most other antagonists, it shows the smallest antagonist induced domain opening seen to date. Thus, our results suggest that compounds may switch from partial agonists to antagonists at GluA2 receptors when domain openings are in the range 11-13°.

Experimental Section

Chemistry

General Procedures. Analytical thin-layer chromatography (TLC) was performed on silica gel 60 F_{254} aluminium plates (Merck). All compounds were detected using UV light and a $KMnO_4$ spraying reagent, and the target amino acids were also visualized using a ninhydrin spraying reagent. Flash column chromatography (FC) was performed using the CombiFlash Companion System (Teledyne Isco, Inc.) on Redi*Sep* columns with silica gel (average particle size 35 to 70 μm). A mixture of heptane and ethyl acetate (both HPLC purity) was used as eluents, unless otherwise stated. ^{1}H NMR spectra were recorded on a 300 MHz Varian Mercury 300BB or 300 MHz Varian Gemini 2000BB spectrometer. ^{13}C NMR spectra were recorded on the Varian Gemini spectrometer. $CDCl_3$, D_2O and

dimethyl-d_6-sulfoxide (DMSO-d_6) were used as solvents. Chemical shifts (δ) are given in parts per million (ppm), and coupling constants (*J*) are given in Hertz (Hz). GC-MS was recorded on a Shimadzu QP 5050A mounted with a Supelco MDN-5S column and chemical ionization was used. Elemental analyses were performed by J. Theiner, Microanalytical Laboratory, Department of Physical Chemistry, University of Vienna, Austria. All target compounds possessed a purity of ≥95% as verified by elemental analyses by comparison with the theoretical values or by UPLC analysis (compound **33**).

Unless otherwise stated, preparative chromatography was performed using HPLC system consisting of a Jasco 880-PU pump, a Rheodyne 7125 injector equipped with a 5.0 mL sample loop, a Shimadzu SPD-6A detector (220 nm or 250 nm) and a Merck-Hitachi D-2000 Chromato-Integrator. Purification of the target racemic amino acids was performed on the reverse-phase XTerra MS C_{18} column (10 × 300 mm, 10 μm, Waters). The column was eluted at 8 mL/min with 15 mM acetic acid containing methanol in varying concentrations depending on the structure of the target amino acid. UPLC analysis was performed using a Waters Acquity UPLC system equipped with a dual wavelength UV detector (observing at 215 and 254 nm) and a QDa single quadropole MS detector operated in positive electro spray mode (ES+) using a Waters Acquity UPLC BEH C18 column (1.7 μm; 2.1 × 50 mm). The column was eluted at 0.3 mL/min with a linear gradient starting at 5% MeCN (aq) to 100% MeCN over 2 minutes followed by one minute of 100% MeCN (total run time 3 min). The mobile phases were supplemented with 0.1 % formic acid.

Preparative chiral separation was performed using Chirobiotic T column (10 × 500 mm, ASTEC) equipped with a Chirobiotic T guard column (4.6 × 50 mm, ASTEC) and connected to the HPLC system described above (detection at 250 nm). Ethanol:water (80:20) was used as mobile phase at 1.5 mL/min. The enantiomeric purity expressed by the enantiomeric excess (ee) was determined by chiral HPLC using an analytical Chirobiotic T column (4.6 × 150 mm, ASTEC) equipped with a Chirobiotic T guard column (4.6 × 50 mm, ASTEC) and connected to the HPLC system described above (detection at 250 nm). Elution was performed with 60% (v/v) ethanol in water adjusted with

acetic acid to pH = 4 at 0.5 mL/min. Analyses of elution orders were carried out using a chiral ligand-exchange column containing (*R*)-Pro as chiral selector and connected to the HPLC system described above (detection at 215 nm). The column was thermostated at 50 °C and eluted with an aqueous solution of KH_2PO_4 (50 mM, pH = 4.5) at 1.0 mL/min. Optical rotation was measured on a Perkin-Elmer 241 polarimeter. CD spectra were recorded at ambient temperature in 1.0 cm cuvettes on an OLIS DSM (Digital Subtractive Method) 10 CD spectrophotometer. Compounds **13** and **14** were prepared as described previously.[26]

General procedure for diethyl 2-acetamido-2-(biphenyl-3-ylmethyl)malonates (15-23, 26) and diethyl 2-acetamido-2-(3-(pyridin-3-yl)benzyl)malonates (24, 25). Compounds **15–26** were prepared in analogy to the known literature method.[33] Suspension of **13** (502 mg, 1 mmol) or **14** (433 mg, 1 mmol) and bis(triphenylphosphine)palladium(II) dichloride $PdCl_2(PPh_3)_2$ (35 mg, 0.05 mmol) was stirred in DME (25 mL) under nitrogen atmosphere at room temperature for 15 min. The adequate boronic acid (or boronic acid pinacol ester) (1.5 mmol), triethylamine (5.58 mL, 40 mmol) and water (25 mL) were added and the mixture was stirred under nitrogen at room temperature for several hours, controlled by GC-MS. If the starting material was not converted after 24 h of stirring, the temperature was raised to 50°C. When the reaction was finished, the mixture was filtrated and water (30 mL) was added. After extraction with ethyl acetate (3×50 mL) the combined extracts were washed with 2M NaOH (50 mL) following water (50 mL), dried ($MgSO_4$) end evaporated. The raw product was purified by flash column chromatography.

*Diethyl 2-acetamido-2-((5,6-dichloro-3',4'-dimethoxybiphenyl-3-yl)methyl)malonate (**15**).* Yield 0.372 g, 73%; ^{1}H NMR (300 MHz, $CDCl_3$): δ 1.28 (t, *J* = 7.2 Hz, 6H, OCH_2CH_3), 2.03 (s, 3H, $NHCOCH_3$), 3.63 (s, 2H, $ArCH_2$), 3.88 (s, 3H, OCH_3), 3.92 (s, 3H, OCH_3), 4.27 (q, *J* = 7.2 Hz, 4H, OCH_2CH_3), 6.57 (s, 1H, NH), 6.85 (d, *J* = 2.2 Hz, 1H, Ar), 6.87-6.91 (m, 3H, Ar), 7.08 (d, *J* = 2.2 Hz, 1H, Ar); ^{13}C NMR (75 MHz, $CDCl_3$): δ 14.5, 23.5, 37.3, 56.2, 56.3, 63.3, 67.3, 111.0, 112.7, 121.7, 130.1, 130.7, 131.3, 131.9, 133.6, 135.0, 142.5, 148.6, 149.0, 167.4, 169.4.

*Diethyl 2-acetamido-2-((5,6-dichloro-3',5'-dimethoxybiphenyl-3-yl)methyl)malonate (**16**).* Yield 0.423 g, 83%; ^{1}H NMR (300 MHz, $CDCl_3$): δ 1.28 (t, *J* = 7.2 Hz, 6H, OCH_2CH_3), 2.03 (s, 3H, $NHCOCH_3$), 3.63 (s, 2H, $ArCH_2$), 3.80 (s, 3H, OCH_3), 3.83 (s, 3H, OCH_3), 4.26 (q, *J* = 7.2 Hz, 4H, OCH_2CH_3), 6.44 (d, *J* = 2.2 Hz, 2H, Ar), 6.47 (t, *J* = 2.2 Hz, 1H, Ar), 6.58 (s, 1H, NH), 6.85 (d, *J* = 2.2 Hz, 1H, Ar), 7.09 (d, *J* = 1.9 Hz, 1H, Ar); ^{13}C NMR (75 MHz, $CDCl_3$): δ 14.5, 23.5, 37.3, 55.8, 63.3, 67.3, 100.3, 107.6, 121.7, 130.2, 130.9, 131.0, 133.5, 135.0, 141.1, 142.7, 160.6, 167.4, 169.5.

*Diethyl 2-acetamido-2-((5,6-dichloro-3'-methoxybiphenyl-3-yl)methyl)malonate (**17**).* Yield 0.357 g, 74%; ^{1}H NMR (300 MHz, $CDCl_3$): δ 1.28 (t, *J* = 7.2 Hz, 6H, OCH_2CH_3), 2.03 (s, 3H, $NHCOCH_3$), 3.63 (s, 2H, $ArCH_2$), 3.82 (s, 3H, OCH_3), 4.26 (dq, J_1 = 7.2 Hz, J_2 = 1.4 Hz, 4H, OCH_2CH_3), 6.58 (s, 1H, NH), 6.85-6.93 (m, 3H, Ar), 7.10 (d, *J* = 1.9 Hz, 1H, Ar), 7.24 (s, 1H, Ar), 7.32 (t, *J* = 7.7 Hz, 1H, Ar); ^{13}C NMR (75 MHz, $CDCl_3$): δ 14.3, 23.3, 37.1, 55.5, 63.1, 67.1, 113.6, 114.9, 121.5, 129.3, 130.1, 130.7, 130.9, 133.5, 134.9, 140.3, 142.4, 159.2, 167.2, 169.3.

*Diethyl 2-acetamido-2-(3,4-dichloro-5-(2,3-dihydrobenzo[b][1,4]dioxin-6-yl)benzyl)malonate (**18**).* Yield 0.416 g, 81%; ^{1}H NMR (300 MHz, $CDCl_3$): δ 1.29 (t, *J* = 7.2 Hz, 6H, OCH_2CH_3), 2.04 (s, 3H, $NHCOCH_3$), 3.63 (s, 2H, $ArCH_2$), 4.23-4.34 (m, 8H, OCH_2CH_3, CH_2 dioxane), 6.58 (s, 1H, NH), 6.79 (dd, J_1 = 8.3 Hz, J_2 = 1.9 Hz, 1H, Ar), 6.83 (d, *J* = 2.2 Hz, 1H, Ar), 7.85 (d, *J* = 1.9 Hz, 1H, Ar), 6.89 (d, *J* = 8.3 Hz, 1H, Ar), 7.07 (d, *J* = 1.9 Hz, 2H, Ar); ^{13}C NMR (75 MHz, $CDCl_3$): δ 14.5, 23.5, 37.3, 63.3, 64.7, 64.8, 67.3, 117.3, 118.4, 122.5, 130.3, 130.6, 131.3, 132.5, 133.5, 135.0, 142.2, 143.3, 143.7, 167.4, 169.5.

*Diethyl 2-acetamido-2-((5,6-dichloro-3'-(hydroxymethyl)biphenyl-3-yl)methyl)malonate (**19**).* Yield 0.366 g, 76%; ^{1}H NMR (300 MHz, $CDCl_3$): δ 1.28 (t, *J* = 7.1 Hz, 6H, OCH_2CH_3), 1.81 (t, *J* = 5.9 Hz, 1H, CH_2OH), 2.03 (s, 3H, $NHCOCH_3$), 3.64 (s, 2H, $ArCH_2$), 4.27 (q, *J* = 7.1 Hz, 4H, OCH_2CH_3), 4.75 (d, *J* = 5.9 Hz, 2H, CH_2OH), 6.61 (s, 1H, NH), 6.87 (d, *J* = 2.1 Hz, 1H, Ar), 7.12 (d, *J* = 2.1 Hz, 1H, Ar), 7.26-7.29 (m, 1H, Ar), 7.34-7.45 (m, 3H, Ar); ^{13}C NMR (75 MHz, $CDCl_3$): δ 14.5, 23.5, 37.3, 63.4, 65.5, 67.3, 126.2, 126.8, 127.9, 128.6, 129.3, 130.9, 131.3, 133.6, 135.2, 139.5, 141.2, 142.6, 167.4, 169.5.

*Diethyl 2-acetamido-2-((5,6-dichloro-4'-(methoxymethyl)biphenyl-3-yl)methyl)malonate (**20**).* Yield 0.433 g, 87%; ^{1}H NMR (300 MHz, $CDCl_3$): δ 1.28 (t, *J* = 7.2 Hz, 6H, OCH_2CH_3), 2.04 (s, 3H, $NHCOCH_3$), 3.46 (s, 3H, OCH_3), 3.65 (s, 2H, $ArCH_2$), 4.27 (dq, J_1 = 7.2 Hz, J_2 = 2.2 Hz, 4H, OCH_2CH_3), 4.51 (s, 2H, CH_2OCH_3), 6.59 (s, 1H, NH), 6.85 (d, *J* = 2.2 Hz, 1H, Ar), 7.12 (d, *J* = 1.9 Hz, 1H, Ar), 7.31 (d, *J* = 8.3 Hz, 1H, Ar), 7.39 (d, *J* = 8.3 Hz, 1H, Ar); ^{13}C NMR (75 MHz, $CDCl_3$): δ 14.3, 23.3, 37.1, 58.6, 63.1, 67.1, 74.5, 127.5, 129.2, 130.1, 130.7, 131.0, 133.3, 134.9, 138.1, 138.3, 142.3, 167.1, 169.3.

*Diethyl 2-acetamido-2-((3'-amino-5,6-dichlorobiphenyl-3-yl)methyl)malonate (**21**).* Yield 0.381 g, 82%; ^{1}H NMR (300 MHz, $CDCl_3$): δ 1.27 (t, *J* = 7.2 Hz, 6H, OCH_2CH_3), 2.02 (s, 3H, $NHCOCH_3$), 3.62 (s, 2H, $ArCH_2$), 3.79 (br.s, 2H, NH_2), 4.26 (dq, J_1 = 7.2 Hz, J_2 = 1.2 Hz, 4H, OCH_2CH_3), 6.64-6.70 (m, 4H, NH, Ar), 6.86 (d, *J* = 2.1 Hz, 1H, Ar), 7.10 (d, *J* = 2.1 Hz, 1H, Ar), 7.18 (t, *J* = 7.8 Hz, 1H, Ar); ^{13}C NMR (75 MHz, $CDCl_3$): δ 14.4, 23.3, 37.2, 63.2, 67.2, 114.9, 115.9, 119.4, 129.3, 130.1, 130.6, 131.0, 133.3, 134.9, 140.2, 142.9, 146.3, 167.1, 169.3.

*Diethyl 2-acetamido-2-((5,6-dichloro-3'-sulfamoylbiphenyl-3-yl)methyl)malonate (**22**).* Yield 0.281 g, 53%; ^{1}H NMR (300 MHz, $CDCl_3$): δ 1.28 (t, *J* = 7.1 Hz, 6H, OCH_2CH_3), 2.05 (s, 3H, $NHCOCH_3$), 3.66 (s, 2H, $ArCH_2$), 4.28 (q, *J* = 7.1 Hz, 4H, OCH_2CH_3), 4.94 (br.s, 2H, SO_2NH_2), 6.63 (s, 1H, NH), 6.88 (d, *J* = 1.8 Hz, 1H, Ar), 7.17 (d, *J* = 1.8 Hz, 1H, Ar), 7.57-7.61 (m, 2H, Ar), 7.89 (s, 1H, Ar), 7.96 (d, *J* = 6.5 Hz, 1H, Ar); ^{13}C NMR (75 MHz, $CDCl_3$): δ 14.3, 23.3, 37.1, 63.3, 67.1, 126.1, 127.2, 129.1, 129.9, 131.0, 131.5, 133.6, 133.7, 135.4, 140.0, 140.6, 142.2, 167.1, 169.6.

*Diethyl 2-acetamido-2-((5,6-dichloro-4'-sulfamoylbiphenyl-3-yl)methyl)malonate (**23**).* Yield 0.336 g, 63%; ^{1}H NMR (300 MHz, $CDCl_3$): δ 1.28 (t, *J* = 7.2 Hz, 6H, OCH_2CH_3), 2.03 (s, 3H, $NHCOCH_3$), 3.66 (s, 2H, $ArCH_2$), 4.27 (q, *J* = 7.2 Hz, 4H, OCH_2CH_3), 4.92 (br.s, 2H, SO_2NH_2), 6.60 (s, 1H, NH), 6.83 (d, *J* = 1.8 Hz, 1H, Ar), 7.18 (d, *J* = 1.8 Hz, 1H, Ar), 7.49 (d, *J* = 8.2 Hz, 2H, Ar), 7.99 (d, *J* = 8.2 Hz, 2H, Ar); ^{13}C NMR (75 MHz, $CDCl_3$): δ 14.3, 23.3, 37.1, 63.2, 67.1, 126.5, 129.9, 130.0, 130.7, 131.7, 133.8, 135.4, 140.7, 141.5, 143.5, 167.1, 169.4.

*Diethyl 2-acetamido-2-(3,4-dichloro-5-(6-methoxypyridin-3-yl)benzyl)malonate (**24**).* Yield 0.426 g, 88%; ^{1}H NMR (300 MHz, $CDCl_3$): δ 1.30 (t, J = 7.2 Hz, 6H, OCH_2CH_3), 2.06 (s, 3H, $NHCOCH_3$), 3.66 (s, 2H, $ArCH_2$), 4.01 (s, 3H, OCH_3), 4.28 (dq, J_1 = 7.2 Hz, J_2 = 2.5 Hz, 4H, OCH_2CH_3), 6.00 (s, 1H, NH), 6.81-6.85 (m, 2H, Ar, pyridine), 7.14 (d, J = 1.7 Hz, 1H, Ar), 7.62 (dd, J_1 = 8.5 Hz, J_2 = 2.5 Hz, 1H, pyridine), 8.13 (d, J = 2.2 Hz, 1H, pyridine); ^{13}C NMR (75 MHz, $CDCl_3$): δ 14.3, 23.3, 37.1, 53.8, 63.2, 67.1, 110.4, 128.0, 130.5, 130.9, 131.1, 133.6, 135.2, 139.1, 139.5, 146.6, 163.7, 167.1, 169.3.

*Diethyl 2-acetamido-2-(3,4-dichloro-5-(5-methoxypyridin-3-yl)benzyl)malonate (**25**).* Yield 0.362 g, 75%; ^{1}H NMR (300 MHz, $CDCl_3$): δ 1.30 (t, J = 7.2 Hz, 6H, OCH_2CH_3), 2.06 (s, 3H, $NHCOCH_3$), 3.68 (s, 2H, $ArCH_2$), 3.92 (s, 3H, OCH_3), 4.29 (dq, J_1 = 7.2 Hz, J_2 = 2.5 Hz, 4H, OCH_2CH_3), 6.61 (s, 1H, NH), 6.87 (d, J = 1.9 Hz, 1H, Ar), 7.18 (d, J = 2.2 Hz, 1H, Ar), 7.53-7.57 (m, 1H, pyridine), 8.18 (d, J = 1.7 Hz, 1H, pyridine), 8.34 (d, J = 2.8 Hz, 1H, pyridine); ^{13}C NMR (75 MHz, $CDCl_3$): δ 14.5, 23.5, 37.3, 56.1, 63.4, 67.3, 121.5, 130.6, 131.1, 131.8, 133.9, 135.4, 135.6, 137.3, 138.9, 142.0, 155.2, 167.3, 169.5.

*Diethyl 2-acetamido-2-((3'-methoxybiphenyl-3-yl)methyl)malonate (**26**).* Yield 0.367 g, 89%; ^{1}H NMR (300 MHz, $CDCl_3$): δ 1.31 (t, J = 7.2 Hz, 6H, OCH_2CH_3), 2.04 (s, 3H, $NHCOCH_3$), 3.72 (s, 2H, $ArCH_2$), 3.86 (s, 3H, OCH_3), 4.29 (dq, J_1 = 7.2 Hz, J_2 = 1.7 Hz, 4H, OCH_2CH_3), 6.58 (s, 1H, NH), 6.88 (dd, J_1 = 8.0 Hz, J_2 = 2.2 Hz, 1H, Ar), 7.00 (d, J = 7.4 Hz, 1H, Ar), 7.05 (t, J = 2.2 Hz, 1H, Ar), 7.10 (d, J = 7.7 Hz, 1H, Ar), 7.21 (s, 1H, Ar), 7.29-7.36 (m, 2H, Ar), 7.46 (d, J = 7.7 Hz, 1H, Ar); ^{13}C NMR (75 MHz, $CDCl_3$): δ 14.3, 23.3, 38.0, 55.4, 62.9, 67.3, 112.7, 112.8, 119.5, 126.1, 128.7, 128.8, 128.9, 129.8, 135.7, 141.1, 142.4, 159.9, 167.5, 169.1.

General procedure for preparation of compounds 2-amino-3-(biphenyl-3-yl)propanoic acids (27-35, 38) and 2-amino-3-(3-(pyridin-3-yl)phenyl)propanoic acids (36, 37). A mixture of **15, 16, 19-26** (0.5 mmol) in 48% aq HBr (6 mL) was refluxed for 2 h. The reaction mixture was evaporated under reduced pressure and purified by reverse-phase HPLC (mobile phase: a mixture of methanol in 15 mM acetic acid) to give white crystals of the final amino acid.

Compounds **17** and **18** were refluxed in a mixture of HCl:water:acetic acid (1:1:1), deprotection was controlled by TLC. After evaporation of solvents the amino acids were purified by reverse-phase HPLC (mobile phase: a mixture of methanol in 15 mM acetic acid) to give white crystals of **29** and **30**, respectively.

*(RS)-2-Amino-3-(5,6-dichloro-3',4'-dihydroxybiphenyl-3-yl)propanoic acid (**27**).* Yield 88 mg, 51%; ^{1}H NMR (300 MHz, DMSO-d_6 + 50 µL D_2O): δ 2.92 (dd, J_1 = 14.4 Hz, J_2 = 7.4 Hz, 1H, $ArCH_2$), 3.10 (dd, J_1 = 14.4 Hz, J_2 = 4.1 Hz, 1H, $ArCH_2$), 3.50-3.54 (m, 1H, $ArCH_2CH$), 6.69 (d, J = 7.9 Hz, 1H, Ar), 6.80 (dd, J_1 = 8.2 Hz, J_2 = 1.8 Hz, 1H, Ar), 6.83-6.84 (m, 1H, Ar), 7.18 (s, 1H, Ar), 7.44 (s, 1H, Ar).

*(RS)-2-Amino-3-(5,6-dichloro-3',5'-dihydroxybiphenyl-3-yl)propanoic acid (**28**).* Yield 82 mg, 48%; ^{1}H NMR (300 MHz, DMSO-d_6 + 50 µL D_2O): δ 2.92 (dd, J_1 = 14.3 Hz, J_2 = 7.7 Hz, 1H, $ArCH_2$), 3.10 (dd, J_1 = 14.4 Hz, J_2 = 4.4 Hz, 1H, $ArCH_2$), 3.51 (dd, J_1 = 7.7 Hz, J_2 = 4.4 Hz, 1H, $ArCH_2CH$), 6.22-6.24 (m, 3H, Ar), 7.16 (d, J = 1.9 Hz, 1H, Ar), 7.46 (d, J = 1.9 Hz, 1H, Ar).

*(RS)-2-Amino-3-(5,6-dichloro-3'-methoxybiphenyl-3-yl)propanoic acid (**29**).* Yield 129 mg, 76%; ^{1}H NMR (300 MHz, DMSO-d_6 + 50 µL D_2O): δ 2.96 (dd, J_1 = 14.4 Hz, J_2 = 7.3 Hz, 1H, $ArCH_2$), 3.14 (dd, J_1 = 14.4 Hz, J_2 = 4.4 Hz, 1H, $ArCH_2$), 3.51-3.58 (m, 1H, $ArCH_2CH$), 3.74 (s, 3H, OCH_3), 6.90-7.00 (m, 3H, Ar), 7.20 (d, J = 2.1 Hz, 1H, Ar), 7.35 (t, J = 7.8 Hz, 1H, Ar), 7.48 (d, J = 1.8 Hz, 1H, Ar).

*(RS)-2-Amino-3-(3,4-dichloro-5-(2,3-dihydrobenzo[b][1,4]dioxin-6-yl)phenyl)propanoic acid (**30**).* Yield 138 mg, 75%; ^{1}H NMR (300 MHz, DMSO-d_6 + 50 µL D_2O): δ 2.92 (dd, J_1 = 14.3 Hz, J_2 = 7.7 Hz, 1H, $ArCH_2$), 3.11 (dd, J_1 = 14.3 Hz, J_2 = 3.9 Hz, 1H, $ArCH_2$), 3.54 (dd, J_1 = 7.7 Hz, J_2 = 4.4 Hz, 1H, $ArCH_2CH$), 6.85-6.92 (m, 3H, Ar), 7.17 (d, J = 1.9 Hz, 1H, Ar), 7.45 (d, J = 1.9 Hz, 1H, Ar).

*(RS)-2-Amino-3-(5,6-dichloro-3'-(hydroxymethyl)biphenyl-3-yl)propanoic acid (**31**).* Yield 102 mg, 60%; ^{1}H NMR (300 MHz, DMSO-d_6 + 50 µL D_2O): δ 2.94 (dd, J_1 = 15.3 Hz, J_2 = 7.3 Hz, 1H,

$ArCH_2$), 3.10-3.14 (m, 1H, $ArCH_2$), 3.54-3.56 (m, 1H, $ArCH_2CH$), 4.52 (s, 2H, CH_2OH), 7.21 (s, 1H, Ar), 7.27-7.43 (m, 4H, Ar), 7.50 (s, 1H, Ar).

*(RS)-2-Amino-3-(5,6-dichloro-4'-(hydroxymethyl)biphenyl-3-yl)propanoic acid (**32**).* Yield 140 mg, 82%; ^{1}H NMR (300 MHz, DMSO-d_6 + 50 µL D_2O): δ 2.94 (dd, J_1 = 14.2 Hz, J_2 = 7.8 Hz, 1H, $ArCH_2$), 3.11-3.15 (m, 1H, $ArCH_2$), 3.49-3.52 (m, 1H, $ArCH_2CH$), 4.53 (s, 2H, CH_2OH), 7.24 (s, 1H, Ar), 7.39-7.40 (m, 4H, Ar), 7.52 (s, 1H, Ar).

*(RS)-2-Amino-3-(3'-amino-5,6-dichlorobiphenyl-3-yl)propanoic acid (**33**).* Yield 60 mg, 37%; ^{1}H NMR (300 MHz, DMSO-d_6 + 50 µL D_2O): δ 2.92 (dd, J_1 = 14.3 Hz, J_2 = 7.7 Hz, 1H, $ArCH_2$), 3.11 (dd, J_1 = 14.3 Hz, J_2 = 4.4 Hz, 1H, $ArCH_2$), 3.50 (dd, J_1 = 7.7 Hz, J_2 = 4.4 Hz, 1H, $ArCH_2CH$), 6.52 (d, J = 7.7 Hz, 1H, Ar), 6.57-6.59 (m, 2H, Ar), 7.07 (t, J = 7.7 Hz, 1H, Ar), 7.16 (d, J = 1.9 Hz, 1H, Ar), 7.46 (d, J = 1.9 Hz, 1H, Ar).

*(RS)-2-Amino-3-(5,6-dichloro-3'-sulfamoylbiphenyl-3-yl)propanoic acid (**34**).* Yield 139 mg, 71%; ^{1}H NMR (300 MHz, DMSO-d_6 + 50 µL D_2O): δ 2.96 (dd, J_1 = 14.1 Hz, J_2 = 7.3 Hz, 1H, $ArCH_2$), 3.13 (dd, J_1 = 14.4 Hz, J_2 = 4.4 Hz, 1H, $ArCH_2$), 3.50-3.54 (m, 1H, $ArCH_2CH$), 7.28 (s, 1H, Ar), 7.59 (s, 1H, Ar), 7.66-7.69 (m, 2H, Ar), 7.86-7.88 (m, 2H, Ar).

*(RS)-2-Amino-3-(5,6-dichloro-4'-sulfamoylbiphenyl-3-yl)propanoic acid (**35**).* Yield 169 mg, 87%; ^{1}H NMR (300 MHz, DMSO-d_6 + 50 µL D_2O): δ 2.96 (dd, J_1 = 14.4 Hz, J_2 = 7.3 Hz, 1H, $ArCH_2$), 3.14 (dd, J_1 = 14.4 Hz, J_2 = 4.4 Hz, 1H, $ArCH_2$), 3.510-3.58 (m, 1H, $ArCH_2CH$), 7.28 (s, 1H, Ar), 7.57 (s, 1H, Ar), 7.63 (dd, J_1 = 8.2 Hz, J_2 = 1.8 Hz, 2H, Ar), 7.90 (dd, J_1 = 8.2 Hz, J_2 = 1.8 Hz, 2H, Ar).

*(RS)-2-Amino-3-(3,4-dichloro-5-(6-hydroxypyridin-3-yl)phenyl)propanoic acid (**36**).* Yield 143 mg, 88%; ^{1}H NMR (300 MHz, DMSO-d_6 + 50 µL D_2O): δ 2.93 (dd, J_1 = 14.3 Hz, J_2 = 7.7 Hz, 1H, $ArCH_2$), 3.11 (dd, J_1 = 14.3 Hz, J_2 = 4.4 Hz, 1H, $ArCH_2$), 3.53 (dd, J_1 = 7.7 Hz, J_2 = 4.4 Hz, 1H, $ArCH_2CH$), 6.44 (d, J = 9.4 Hz, 1H, pyridine), 7.23 (d, J = 2.2 Hz, 1H, Ar), 7.47 (d, J = 1.9 Hz, 1H, Ar), 7.50 (d, J = 2.2 Hz, 1H, pyridine), 7.60 (dd, J_1 = 9.6 Hz, J_2 = 2.8 Hz, 1H, pyridine).

*(RS)-2-Amino-3-(3,4-dichloro-5-(5-hydroxypyridin-3-yl)phenyl)propanoic acid (**37**).* Yield 143 mg, 88%; ^{1}H NMR (300 MHz, DMSO-d_6 + 50 μL D_2O): δ 2.94 (dd, J_1 = 14.1 Hz, J_2 = 7.5 Hz, 1H, $ArCH_2$), 3.12 (dd, J_1 = 14.1 Hz, J_2 = 4.2 Hz, 1H, $ArCH_2$), 3.55-3.58 (m, 1H, $ArCH_2CH$), 7.21-7.25 (m, 2H, Ar, pyridine), 7.53 (s, 1H, Ar), 8.04 (s, 1H, pyridine), 8.12 (s 1H, pyridine).

*(S)-(+)- and (R)-(–)-2-amino-3-(3,4-dichloro-5-(5-hydroxypyridin-3-yl)phenyl)propanoic acid [(S)-(+)- and (R)-(–)-(**37**)]*. Racemic **37** dissolved in EtOH: H_2O (1:1) (110 mg; 10 mg/mL) was separated by chiral HPLC using a semi-preparative Chirobiotic T column in 10 mg injections. Fractions containing the first-eluting (+)-**37** isomer were pooled, evaporated and recrystallized from water to give (+)-**37** (27 mg, 49%); mp 234 – 249 °C (dec.); $[\alpha]_D^{20}$ +19.3 [*c* 0.22, EtOH:$HCl_{(aq)}$ (0.25 M) (1:1)]; ee > 97%. ^{1}H NMR (300 MHz, DMSO-d_6): δ 2.94 (dd, J_1 = 14.1 Hz, J_2 = 7.2 Hz, 1H, $ArCH_2$), 3.08 (dd, J_1 = 14.1 Hz, J_2 = 4.5 Hz, 1H, $ArCH_2$), 3.51 (dd, J_1 = 7.2 Hz, J_2 = 4.5 Hz, 1H, $ArCH_2CH$), 7.22 (dd, J_1 = 2.7 Hz, J_2 = 1.8 Hz, 1H, Ar), 7.27 (d, J = 1.8 Hz, 1H, Ar), 7.56 (d, J = 1.8 Hz, 1H, Ar), 8.06 (d, J = 1.5 Hz, 1H, Ar), 8.15 (d, J = 2.4 Hz, 1H, Ar).

Fractions containing the second-eluting (–)-**37** isomer were pooled, evaporated and recrystallized from water to give (–)-**37** (34 mg, 62%); mp 236 – 242 °C (dec.); $[\alpha]_D^{22}$ –19.2 [*c* 0.22, EtOH:$HCl_{(aq)}$ (0.25M) (1:1)]; ee = 99.7%. ^{1}H NMR (300 MHz, DMSO-d_6) was identical with that of (+)-**37**.

*(RS)-2-Amino-3-(3'-hydroxybiphenyl-3-yl)propanoic acid (**38**).* Yield 92 mg, 52%; ^{1}H NMR (300 MHz, DMSO-d_6 + 50 μL D_2O): δ 2.93 (dd, J_1 = 14.3 Hz, J_2 = 8.3 Hz, 1H, $ArCH_2$), 3.19 (dd, J_1 = 14.2 Hz, J_2 = 3.9 Hz, 1H, $ArCH_2$), 3.52 (dd, J_1 = 8.3 Hz, J_2 = 4.1 Hz, 1H, $ArCH_2CH$), 6.73 (dd, J_1 = 8.0 Hz, J_2 = 1.4 Hz, 1H, Ar), 7.00-7.01 (m, 1H, Ar), 7.06 (d, J = 8.0 Hz, 1H, Ar), 7.20-7.25 (m, 2H, Ar), 7.34 (t, J = 7.7 Hz, 1H, Ar), 7.43 (d, J = 8.0 Hz, 1H, Ar), 7.47 (s, 1H, Ar).

General procedure for preparation of (S)- and (R)-ethyl 2-(tert-butoxycarbonylamino)-3-(3'-methoxybiphenyl-3-yl)propanoates (41, 42). The compounds **41** and **42** were prepared from *S*- and *R*-isomers of ethyl 3-(3-bromophenyl)-2-(tert-butoxycarbonylamino)propanoate (242 mg, 0.65 mmol) and 3-methoxyphenylboronic acid according to the procedure described for compounds **15-26**.

*(S)-Ethyl 2-(tert-butoxycarbonylamino)-3-(3'-methoxybiphenyl-3-yl)propanoate (**41**).* Yield 228 mg, 89%; ^{1}H NMR (300 MHz, $CDCl_3$): δ 1.22 (t, *J* = 7.2 Hz, 3H, OCH_2CH_3), 1.41 (s, 9H, CH_3), 3.15-3.17 (m, 2H, $ArCH_2$), 3.87 (s, 3H, OCH_3) 4.16 (q, *J* = 7.1 Hz, 2H, OCH_2CH_3), 4.61 (d, *J* = 7.1 Hz, 1H, *CH*NH), 5.03 (d, *J* = 7.1 Hz, NH), 6.89-6.91 (m, 1H, Ar), 7.10-7.16 (m, 3H, Ar), 7.32-7.38 (m, 3H, Ar), 7.46 (d, *J* = 7.6 Hz, 1H, Ar); ^{13}C NMR (75 MHz, $CDCl_3$): δ 14.4, 28.5, 38.6, 54.6, 55.5, 61.6, 80.1, 112.8, 112.9, 119.9, 125.9, 128.4, 128.4, 128.9, 129.8, 136.6, 141.8, 142.5, 155.5, 159.9, 171.8.

*(R)-Ethyl 2-(tert-butoxycarbonylamino)-3-(3'-methoxybiphenyl-3-yl)propanoate (**42**).* Yield 221 mg, 86%; ^{1}H NMR (300 MHz, $CDCl_3$): δ 1.22 (t, *J* = 7.2 Hz, 3H, OCH_2CH_3), 1.41 (s, 9H, CH_3), 3.13-3.17 (m, 2H, $ArCH_2$), 3.87 (s, 3H, OCH_3), 4.16 (q, *J* = 7.1 Hz, 2H, OCH_2CH_3), 4.60 (d, *J* = 7.1 Hz, 1H, *CH*NH), 5.03 (d, *J* = 7.1 Hz, NH), 6.88-6.91 (m, 1H, Ar), 7.10-7.16 (m, 3H, Ar), 7.32-7.38 (m, 3H, Ar), 7.46 (d, *J* = 7.6 Hz, 1H, Ar); ^{13}C NMR (75 MHz, $CDCl_3$): δ 14.4, 28.5, 38.6, 54.6, 55.5, 61.6, 80.1, 112.8, 112.9, 119.7, 125.9, 128.4, 128.4, 128.9, 129.8, 136.6, 141.8, 142.5, 155.5, 159.9, 171.8.

General procedure for preparation of (S)- and (R)-2-amino-3-(3'-hydroxybiphenyl-3-yl)propanoic acids. The target amino acids (*S*)-**38** and (*R*)-**38** were obtained from **41** and **42**, respectively (197 mg, 0.5 mmol) according to the procedure described for compounds **27, 28** and **31-38**, followed by two-time recrystallization from water.

*(S)-2-Amino-3-(3'-hydroxybiphenyl-3-yl)propanoic acid ((S)-**38**).* Yield 53 mg, 41%; ee = 98.3%; $[\alpha]_D^{22}$ +25.4° [*c* 0.014, 1M HCl:EtOH (1:1)]; Δε (214 nm) = +0.044 m^2/mol; ^{1}H NMR (300 MHz, DMSO-d_6): δ 2.94-2.97 (m, 1H, $ArCH_2$), 3.20 (d, *J* = 14.9 Hz, 1H, $ArCH_2$), 3.45 (m, 1H, $ArCH_2CH$), 6.75 (d, *J* = 7.3 Hz, 1H, Ar), 7.05-7.08 (m, 2H, Ar), 7.20-7.26 (m, 2H, Ar), 7.34 (t, *J* = 7.6 Hz, 1H, Ar), 7.43 (d, *J* = 8.2 Hz, 1H, Ar), 7.51 (s, 1H, Ar).

*(R)-2-Amino-3-(3'-hydroxybiphenyl-3-yl)propanoic acid ((R)-**38**).* Yield 34 mg, 26%; ee = 98.0%; $[\alpha]_D^{22}$ –24.5° [*c* 0.014, 1M HCl:EtOH (1:1)]; Δε (212 nm) = –0.038 m^2/mol; ^{1}H NMR (300 MHz, DMSO-d_6 + 50 μL D_2O): δ 2.90-2.97 (m, 1H, $ArCH_2$), 3.17-3.22 (m, 1H, $ArCH_2$), 3.53 (dd, J_1 = 7.9

Hz, J_2 = 4.1 Hz, 1H, $ArCH_2CH$), 6.73 (d, J = 8.2 Hz, 1H, Ar), 7.02 (s, 1H, Ar), 7.07 (d, J = 7.6 Hz, 1H, Ar), 7.22-7.25 (m, 2H, Ar), 7.33-7.37 (m, 1H, Ar), 7.44 (d, J = 7.6 Hz, 1H, Ar), 7.48 (s, 1H, Ar).

Pharmacology

Receptor binding assays using native rat brain homogenates. Rat brain membrane preparations used in the native receptor binding experiments were prepared according to the method described by Ransom and Stec.[34] Affinity for AMPA,[35] KA[36] and NMDA[37] receptor sites was determined using 5 nM [^{3}H]AMPA, 5 nM [^{3}H]KA, and 2 nM [^{3}H]CGP 39653 (Perkin Elmer) with some modifications as previously described.[38]

Recombinant rat AMPA and KA receptor binding assays. $GluA1_o$, $GluA2(R)_o$, $GluA3_o$, $GluK1(Q)_{1b}$, GluK2(*V,C,R*)A and GluK3A were inserted into recombinant baculoviruses, receptors expressed by infection of *Sf9* insect cells and infected *Sf9* cell membranes utilized for radioligand binding assays. $GluA1_o$–4_o were assayed using [^{3}H]-AMPA radioligand while $GluK1(Q)_{1b}$, GluK2(*V,C,R*) and GluK3A receptor binding assays were carried out using [^{3}H]-SYM 2081 radioligand as previously detailed.[38, 39]

GluA2 LBD binding assay. Purified soluble GluA2 LBD (GluR2-S1S2J; 50 ng) was incubated with 1-3 nM [^{3}H]-AMPA in the presence of competing ligand for 2 h at 4°C in 0.25 mL assay buffer (50 mM Tris-HCl, 100 mM KSCN, 2.5 mM $CaCl_2$, 10% (v/v) glycerol, pH 7.2 at 4°C). Samples were diluted with 1 mL ice-cold assay buffer, immediately filtered onto 25 mm 0.2 μM mixed cellulose ester filters (Tisch Scientific, Cleves, OH) and washed once with 1 mL ice-cold assay buffer. Filters were dried 1 h at 70°C and then dissolved in 2 mL Filter-Count (PerkinElmer) and radioactivity determined by liquid scintillation counting (TriCarb 2900, PerkinElmer). Data were analyzed using GraphPad Prism v6 (GraphPad Software, San Diego, CA). The K_d value of [^{3}H]AMPA at GluA2 LBD (12.8 nM) was previously determined.[31]

TEVC pharmacology. Surgical procedures were conducted under the approval of the Danish Ministry of Justice Animal Experiments Inspectorate. Mature female *Xenopus lævis* were

anaesthetized using 0.1% ethyl 3-aminobenzoate methanesulfonate (tricaine) and ovaries were surgically removed. The ovarian tissue was dissected and treated with 2 mg/mL collagenase in nominally Ca^{2+}-free Barth's medium (in mM: 88 NaCl, 1 KCl, 0.33 $Ca(NO_3)_2$, 0.41 $CaCl_2$, 0.82 $MgSO_4$, 2.4 $NaHCO_3$, 10 HEPES, pH 7.4) for 2 h at room temperature. On the second day, oocytes were injected with 25-50 nL of (≈ 1 mg/mL) rat GluA2(Q)$_i$ cRNA and incubated in Barth's medium with 0.10 mg/mL gentamicin (Sigma Chemical) and 1% penicillin-streptomycin (Life Technologies, Paisley, UK) at 17°C. Oocytes were typically used for recordings from 3 to 10 days post-injection and were voltage-clamped with the use of a two-electrode voltage clamp (GeneClamp 500B, Axon Instruments, Union City, CA) with both microelectrodes filled with 3 M KCl. Recordings were made while the oocytes were continuously superfused with frog Ringer's solution (in mM: 115 NaCl, 2 KCl, 1.8 $BaCl_2$, 5 HEPES, pH 7.6). Drugs were dissolved in frog Ringer's solution and added by bath application. Recordings were made at room temperature. Efficacy measurements were made at GluA2(Q)$_i$ in the presence of 100 μM cyclothiazide in order to block receptor desensitization (cyclothiazide EC_{50} at GluA2(Q)$_i$ = 7.6 μM.)[40] To determine the maximum response, oocytes were stimulated with 1 mM (*S*)-glutamate plus 100 μM cyclothiazide. Concentration-response curves of antagonists made in the presence of 10 μM (*S*)-Glu were analyzed using GraphPad Prism v6 (Graphpad Software Inc., San Diego, CA) to determine the IC_{50} and Hill value (n_H), using a four parameter logistic equation. K_b was calculated from the IC_{50} value by the Cheng-Prusoff equation. Homomeric GluA2(Q)$_i$ was expressed in *Xenopus laevis* oocytes and channel activity measured as previously described.[41] Concentration-response curves of (*S*)-**37** inhibition of 10 μM (*S*)-Glu responses were fit to a logistic equation to determine slope (n_H) and IC_{50}, from which K_b was calculated using the Cheng-Prusoff equation.

Structure determination

Crystallization of GluA2 LBD in complex with (S)-37. The rat GluA2 LBD (GluR2-S1S2J[19]) was expressed and purified essentially as previously described.[42, 43] GluA2 LBD in complex with (*S*)-**37**

was crystallized using the hanging drop vapor diffusion method at 7 °C. The drop contained 1 μL of the complex solution (5.5 mg/mL GluA2 LBD in 10 mM HEPES pH 7.0, 20 mM NaCl and 1 mM EDTA equilibrated with the ligand (*S*)-**37** as solid compound) and 1 μL of reservoir solution of 20% PEG4000, 0.3 M Li_2SO_4 and 0.1 M phosphate-citrate pH 4.5. Reservoir volume was 0.5 mL. The crystals appeared within one week and were flash cooled in liquid nitrogen after soaking in cryo buffer consisting of the reservoir solution with 20% glycerol added.

Crystallization of GluA2 LBD in complex with (R)-38. Crystallization of GluA2 LBD with (*R*)-**38** was carried out by the hanging drop vapor diffusion method at 7 °C. The complex solution contained 8.5 mg/mL GluA2 LBD (in 10 mM HEPES, 20 mM NaCl and 1 mM EDTA, pH 7.0) equilibrated with (*R*)-**38** as solid compound. Crystals were grown in drops of 1 μL complex solution and 1 μL reservoir solution of 16% PEG2000, 0.1 M Li_2SO_4 and 0.1 M phosphate-citrate buffer pH 4.5. The reservoir volume was 0.5 mL. The crystals appeared within one week, and were flash cooled in liquid nitrogen after soaking in cryo buffer consisting of the reservoir solution including 8% glycerol, 8% ethylene glycol, 9% sucrose and 2% glucose.

Data collection and processing. X-ray data of the GluA2 LBD in complex with (*S*)-**37** were collected at the ID23-2 beamline (ESRF, Grenoble, France) at a wavelength of 0.8726 Å to 2.0 Å resolution. Data processing was performed with the CCP4i suite of programs.[44] The data of the GluA2 LBD in complex with (*R*)-**38** were collected at the I911-3 beamline (MAX-Lab, Lund, Sweden) at a wavelength of 1.0000 Å to 1.8 Å resolution. Data processing was performed with XDS[45] and scaling using the CCP4 suite of programs.

Both structure determinations were carried out by molecular replacement using the program PHASER[46] implemented in CCP4i. The GluA2 LBD with (*S*)-ATPO (PDB ID 1N0T, molA[9]) was used as a search model, including protein atoms only. Clear solutions were found, showing one molecule in the asymmetric unit for the complex with (*S*)-**37** and four molecules in the asymmetric unit of the complex with (*R*)-**38**. Subsequently, the amino acid residues of the GluA2 complex were automatically built using ARP/wARP within CCP4i except for a few residues, which were manually

built using COOT.[47] The ligand coordinates were created in Maestro[48] and fitted into the electron density. Topology and parameter files for (*S*)-**37** and (*R*)-**38** were obtained using eLBOW[49], keeping geometry after ligand optimization in MacroModel (MMFF94s).[50] The two structures were refined using PHENIX,[51] and between refinements the model was inspected and corrected in COOT. (*S*)-**37**, (*R*)-**38**, water, ethylene glycol and glycerol molecules, as well as chloride and sulfate ions, were manually modelled into the electron densities. Both structures were validated using tools in PHENIX and COOT. For statistics on data collection and refinements, see Table 3.

Structure Analysis. Domain opening of GluA2 LBD in complex with (*S*)-**37** and (*R*)-**38**, both relative to the structure of GluA2 LBD with Glu (PDB ID 1FTJ, molB[19]) was calculated using the DynDom Server.[52] Figures were prepared in PyMOL.[53]

Molecular docking studies

The two protein-ligand complexes (GluA2 LBD in complex with (*S*)-**37** and (*R*)-**38**, respectively) were prepared with the Protein Preparation Wizard in Maestro from Schrodinger (Maestro, version 9.5, Schrödinger, LLC, New York, NY, 2013). The A chain and the ligand were kept for each of the protein-ligand complexes. Default settings were applied for the preparation, except that only the positions of the hydrogen atoms were optimized in the final refinement step. Prior to docking the new ligands, they were optimized with Macromodel (MacroModel, version 10.1, Schrödinger, LLC, New York, NY, 2013) using default settings (i.e. with the OPLS-2005 force field in water).

A conformational search was carried out using the Monte Carlo multiple minimization (MCMM) approach implemented in Macromodel. Default settings were applied for the conformational search. A constrained minimization of the ligand, in the conformation as when bound to the protein, was done. All non-polar hydrogen atoms were free in the minimization while the heavy atoms and the polar hydrogen atoms were constrained by using a force constant of 100.0 kJ/mol/Å^2 and well-size of 0.3 Å in a flat-bottom potential. The strain of the docked ligands was determined as the energy

difference from the constrained minimization and the MCMM calculation. The amino acid moiety of the ligands was not considered in the calculations. All docking were performed with the XP version of Glide (Glide, version 6.0, Schrödinger, LLC, New York, NY, 2013).[54-56] Compounds were docked in the tautomer form and protonation state shown in Table 1, except for **36** that was docked in its pyridone tautomer form. All water molecules were removed. The receptor grid was generated using default settings, except that the size of the enclosing box was increased to 16 Å x 16 Å x 16 Å around the ligand and the hydroxyl groups of Thr655, Thr686 and Tyr702 were allowed to be flexible. Sitemaps of the two proteins were generated using Sitemap (SiteMap, version 2.9, Schrödinger, LLC, New York, NY, 2013). The ligands were used as center in the calculations.

Figure legends

Figure 1. Structures of selected competitive antagonists of AMPA and kainate receptors.

Figure 2. (A) Structures of the most active previously obtained phenylalanines. **(B)** Structures of the present target compounds.

Figure 3. Antagonism of 10 μM (*S*)-Glu responses at GluA2(Q)$_i$ receptors recorded by TEVC in *X. lævis* oocytes. Shown are means ± SEM of pooled data from eight normalized experiments, conducted in duplicate. (*S*)-**37** IC_{50} = 3.7 μM. *Inset:* Sample trace from one experiment at V_h = -60 mV with duplicate stimulations of 10 μM (*S*)-Glu + (*S*)-**37** (in μM): zero, 0.01, 0.03, 0.1, 0.3, 1, 3, 10, 30, 100. Scale bars are 250 nA and 5 min. (*R*)-**38** IC_{50} = 6.3 μM. *Inset:* Sample trace from one experiment at V_h = -70 mV with duplicate stimulations of 10 μM (*S*)-Glu + (*R*)-**38** (in μM): zero, 0.01, 0.1, 0.3, 1, 3, 10, 30, 100, 300. Scale bars are 100 nA and 10 min.

Figure 4. Structures of GluA2 LBD in complex with (*S*)-**37** (**A-C**) and (*R*)-**38** (**D-F**), respectively. (**A)** Cartoon representation of the GluA2 LBD dimer (in dark salmon) in complex with (*S*)-**37** (in yellow). The degree of domain opening induced by (*S*)-**37** as well as the Ile633-Ile633 linker-linker distance is indicated on the figure. (**B**) Zoom on the ligand binding site of GluA2 LBD with (*S*)-**37** bound. A $2F_o$-F_c omit map at 1 σ carved around the ligand at 1.6 Å radius is shown. Potential hydrogen bonds within 3.2 Å to water molecules (red spheres) and surrounding residues are shown as black, dashed lines. Residues within 4.0 Å distance from chlorine atoms have been included. (**C**) Zoom on the cavity accommodating the pyridine ring system of (*S*)-**37**. (GOL, glycerol) (**D**) Cartoon representation of the GluA2 LBD dimer (in dark salmon) in complex with (*R*)-**38** (in cyan). The degree of domain opening induced by (*R*)-**38** as well as the Ile633-Ile633 linker-linker distance is indicated on the figure. (**E**) Zoom on the ligand binding site of GluA2 LBD with (*R*)-**38** bound. A $2F_o$-F_c omit map at

1 σ carved around the ligand at 1.6 Å radius is shown. Potential hydrogen bonds within 3.2 Å to water molecules (red spheres) and surrounding residues are shown as black, dashed lines. (**F**) Zoom on the new cavity near the D1-D2 hinge region accommodating the phenoxy group of (*R*)-**38**. Residues within 4 Å are shown (for visibility Thr482 and Ser654 are not shown).

Figure 5. SiteMaps of the ligand binding sites. The red, blue and brown surfaces show the hydrogen bonding acceptor (at –10 kcal/mol), donor (–10 kcal/mol), and hydrophobic (–0.5 kcal/mol) regions, respectively, for (*S*)-**37** (left) and (*R*)-**38** (right).

Figure 6. Comparison of all antagonists determined in complex with GluA2 LBD (PDB IDs 4ISU, 4GXS, 3TZA, 3UA8, 3R7X, 3KGC, 3H06, 3H03, 3BKI, 3B7D, 2CMO, 1N0T, 1FTL). The structures were superimposed on the D1 residues. (**A**) A new cavity is opened by (*R*)-**38** (in cyan). (*S*)-**37** (in yellow) binds like most other antagonists (light grey). (**B**) Superimposition of (*S*)-**37** and (*R*)-**38** illustrating the difference in binding modes.

Scheme 1. (i) NBS, benzoyl peroxide, CCl_4, reflux; (ii) NaH, diethyl acetamidomalonate, DMF, r.t.; (iii) substituted phenylboronic acid or 2-/3-methoxypyridine-5-boronic acid or boronic acid pinacol ester, $PdCl_2(PPh_3)_2$, triethylamine, DME:water (1:1), r.t.; (iv) 48% HBr, reflux.

Scheme 2. (i) C_2H_5I, $NaHCO_3$, DMF, r.t.; (ii) 3-methoxyphenylboronic acid, $PdCl_2(PPh_3)_2$, triethylamine, DME:water (1:1), r.t.; (iii) 48% HBr, reflux.

Figure 1

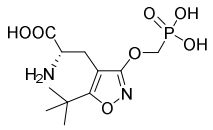

(*S*)-ATPO (**1**)

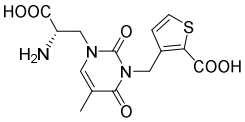

UBP310 (**2**)

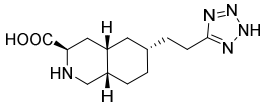

tezampanel (**3**)

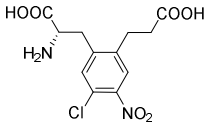

(**4**)

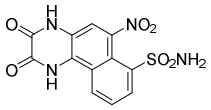

NBQX (**5**)

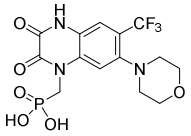

ZK-200775 (**6**)

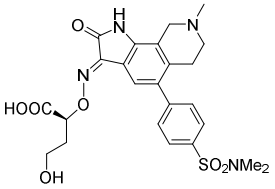

NS1209 (**7**)

Figure 2

A

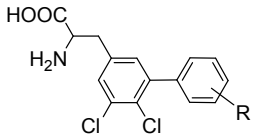

R = 2-OH (**8**), 3-OH (**9**), 4-OH (**10**)

B

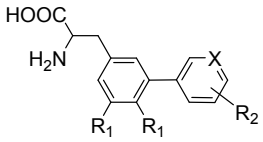

X = C, N
R_1 = H, Cl
R_2 = OH, diOH, CH_2OH, NH_2, SO_2NH_2, OCH_3

Figure 3

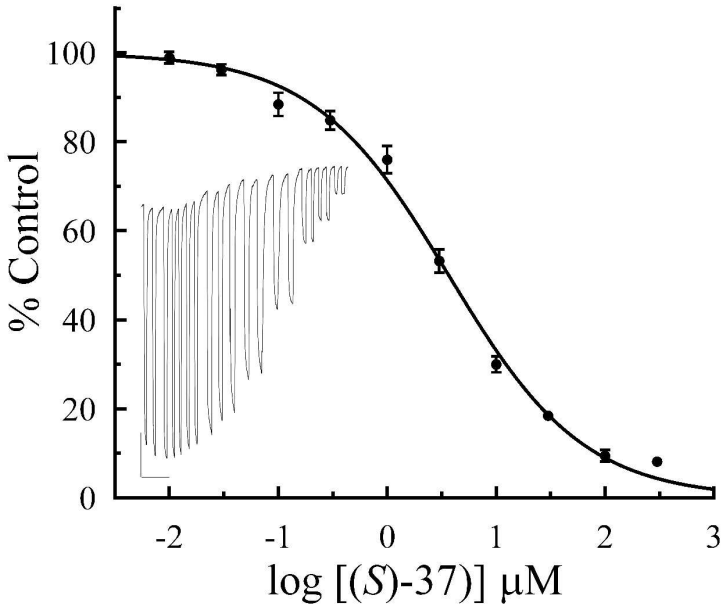
100
80
60
40
20
0
% Control
-2
-1
0
1
2
3
log [(S)-37)] μM

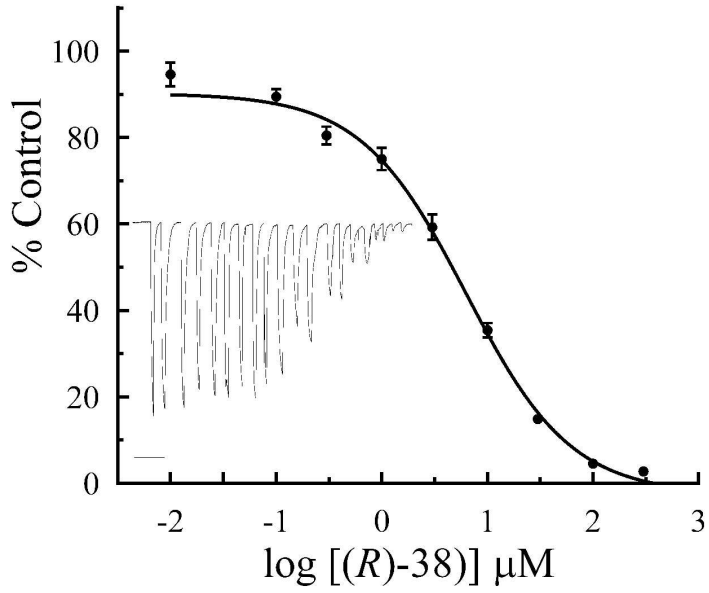
100
80
60
40
20
0
% Control
-2
-1
0
1
2
3
log [(R)-38)] μM

Figure 4

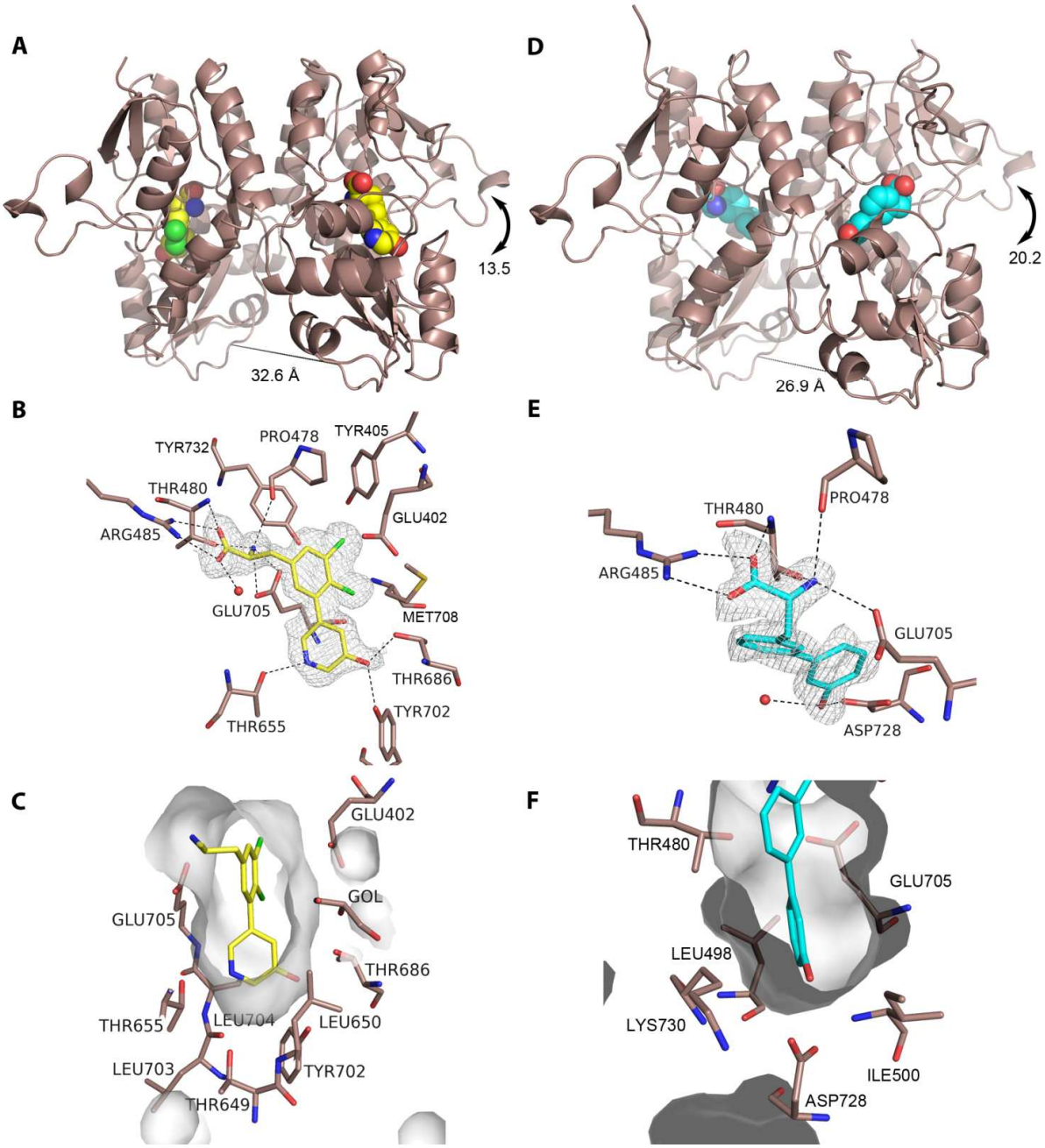
A
13.5
32.6 Å
D
20.2
26.9 Å
B
TYR732
PRO478
TYR405
THR480
GLU402
ARG485
GLU705
MET708
THR686
TYR702
THR655
E
THR480
PRO478
ARG485
GLU705
ASP728
C
GLU402
GOL
GLU705
THR686
THR655
LEU704
LEU650
LEU703
TYR702
THR649
F
THR480
GLU705
LEU498
LYS730
ILE500
ASP728

Figure 5

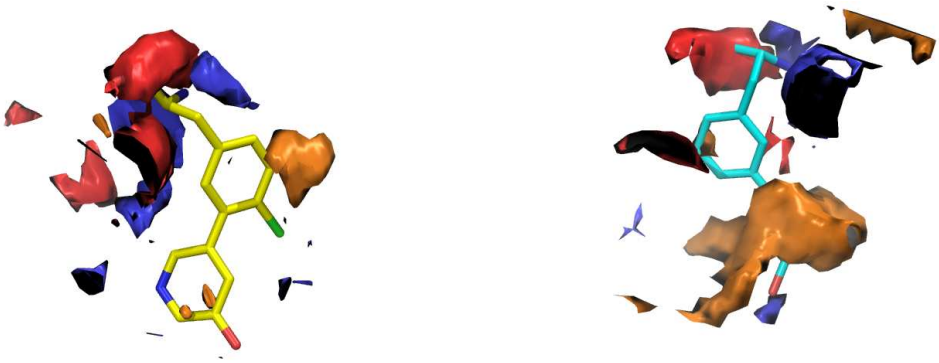

Figure 6

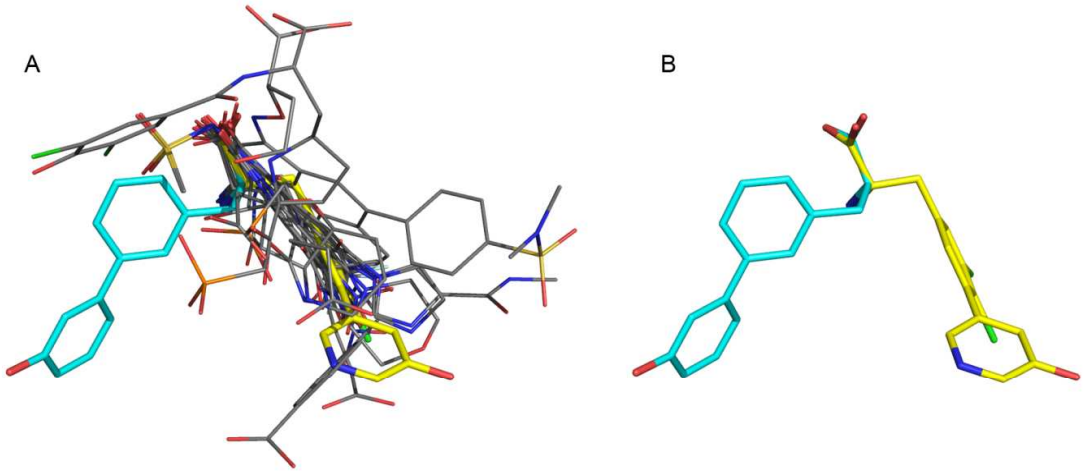

Scheme 1

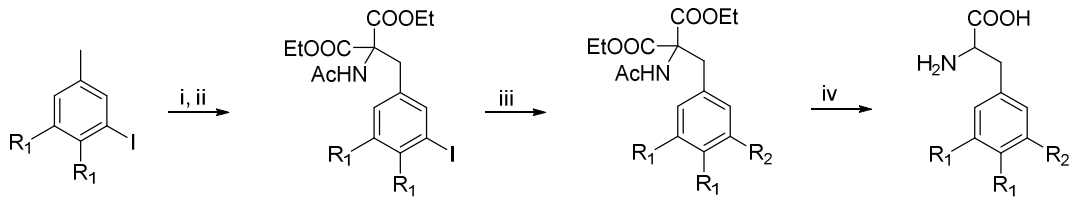

11: R_1 = Cl
12: R_1 = H

13: R_1 = Cl
14: R_1 = H

15–26

27–38

Scheme 2

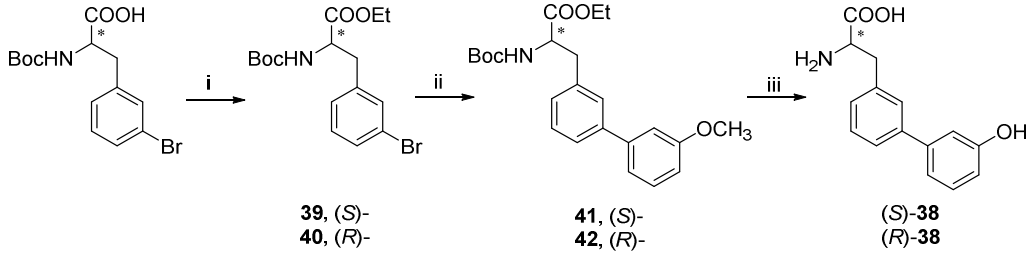

39, (*S*)-
40, (*R*)-

41, (*S*)-
42, (*R*)-

(*S*)-**38**
(*R*)-**38**

Table 1. Binding affinities at native AMPA receptors

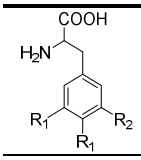	R_1	R_2	IC_{50} (μM) [^{3}H]AMPA
8[26]	Cl		85 ± 1
9[26]	Cl	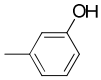	4.6 ± 0.2
10[26]	Cl	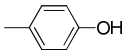	33 ± 4
27	Cl	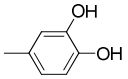	12 ± 2
28	Cl	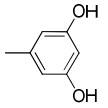	16 ± 3
29	Cl	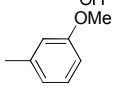	> 100
30	Cl	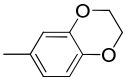	> 100
31	Cl	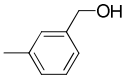	> 10
32	Cl	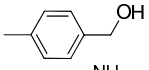	> 10
33	Cl	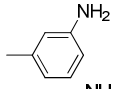	> 100
34	Cl	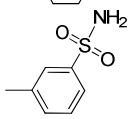	> 100
35	Cl	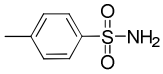	> 100
36	Cl	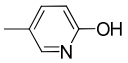	> 100
37	Cl	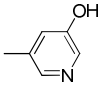	1.5 ± 0.1
(*S*)-**37**	Cl	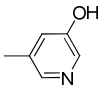	0.67 ± 0.03
(*R*)-**37**	Cl	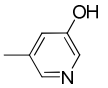	>100
38	H	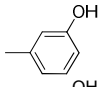	9.9 ± 2.2
(*S*)-**38**	H	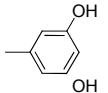	> 100
(*R*)-**38**	H	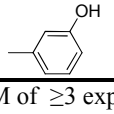	8.3 ± 0.5

Shown are means ± SEM of ≥3 experiments conducted in triplicate.

Table 2. Binding affinities of selected compounds at recombinant AMPA and kainate receptors and functional pharmacology of selected compounds at GluA2

	Receptor binding						Functional
Compound	GluA1 K_i (μM)	GluA2 K_i (μM)	GluA3 K_i (μM)	GluK1 K_i (μM)	GluK2 K_i (μM)	GluK3 K_i (μM)	GluA2(Q)$_i$ K_b (μM)
(*RS*)-**9**	17.1 ± 4.5	5.03 ± 0.41	55.1 ± 12.2	92.3 ± 2.3	78.1 ± 9.8	52.3 ± 2.6	13.6 ± 1.1[a]
(+)-(*S*)-**37**[d]	6.65 ± 0.36[b]	1.74 ± 0.18[b]	6.88 ± 0.46[b]	> 100	> 100	> 100	1.80 ± 0.57[a,c]
(−)-(*R*)-**37**	> 100	> 100	> 100	> 100	> 100	> 100	–
(+)-(*S*)-**38**	> 100	> 100	> 100	> 100	> 100	> 100	–
(−)-(*R*)-**38**[e]	54.1 ± 2.9	24.0 ± 5.2	54.7 ± 2.1	105 ± 22	136 ± 22	39.6 ± 1.1	3.90 ± 0.54[a]

Shown are means ± SEM of n ≥ 3 experiments conducted in triplicate (K_i) and means ± SEM of n = 8 experiments conducted in duplicate (K_b).

[a] No agonist response observed in the presence of 0.1 mM cyclothiazide. [b] GluA1 and GluA3 statistically significantly different from GluA2 ($P < 0.0001$, one-way ANOVA with Holm-Sidak post-test). However, GluA1 is not different from GluA3. [c] Not statistically different from radioligand binding K_i at full length GluA2(R)$_o$ ($P = 0.949$, t-test). [d] Binding affinity at GluA2 LBD: K_i = 2.26 ± 0.28 μM which is not statistically different from full length GluA2(R)$_o$. [e] Binding affinity at GluA2 LBD: K_i = 84 ± 7 μM. (– : not determined).

Table 3. Data collection and refinement statistics of GluA2 LBD crystallized with (*S*)-**37** and (*R*)-**38**

Data	**GluA2 LBD**: (*S*)-**37**	**GluA2 LBD:** (*R*)-**38**
Beamline	ID23 (ESRF)	I911-3 (MAX-lab)
Space group	$P2_12_12$	$P2_12_12_1$
Unit cell dimensions		
a (Å)	60.13	61.47
b (Å)	95.78	92.20
c (Å)	49.42	197.48
Molecules (a.u.)[a]	1	4
Resolution (Å)	38.18 – 2.00 (2.10-2.00)[b]	29.53 – 1.80 (1.90 – 1.80)[b]
Unique reflections	19935 (2791)	96675 (13518)
Average redundancy	3.2 (3.2)	4.4 (2.2)
Completeness (%)	99.3 (97.7)	92.5 (90.6)[c]
R_{merge} (%)[d]	8.2 (33.6)	7.4 (26.5)
I/σ(I)	6.3 (2.2)	5.6 (2.0)
Refinement		
Amino acid residues	258	260/259/261/262
Ligand molecules	1	4
Sulfate/chloride/acetate	6/-/1	10/1/-
Water/glycerol/ethylene glycol	162/3/-	1406/4/14
R_{work} (%)[e]/R_{free} (%)[f]	18.6/23.8	16.7/21.9
Average B-values (Å^2) for:		
Amino acid residues	23.9	11.9/12.2/12.6/12.2
Ligand	18.9	7.1/8.0/9.8/8.0
Sulfate/chloride/acetate	52.9/-/39.6	41.4/53.3/-
Water/glycerol/ethylene glycol	28.1/29.4/-	20.2/30.7/22.8
R.M.S. deviation bond length (Å)/angles (degrees)	0.007/1.1	0.006/1.0
Residues in allowed regions of Ramachandran plot (%)[g]	100.0	100.0

[a] a.u.: asymmetric unit.
[b] Numbers in parentheses are for the outermost bin.
[c] A completeness of 92.5% is due to ice rings.
[d] A measure on agreement among multiple measurements of the same reflections. R_{merge} is calculated as follows: $I_i(hkl)$ is the intensity of an individual measurement of the reflection with Miller indices hkl, and I(hkl) is the intensity from multiple observations:

$$R_{merge} = \Sigma_{hkl} \Sigma_i |I_i(hkl) - I(hkl)| / \Sigma_{hkl} \Sigma_i |I_i(hkl)|$$

[e] $R_{work} = \Sigma_{hkl} (||F_{o,hkl}| - |F_{c,hkl}||)/|F_{o,hkl}|$, where $|F_{o,hkl}|$ and $|F_{c,hkl}|$ are the observed and calculated structure factor amplitudes.
[f] R_{free} is equivalent to R_{work}, but calculated with 5% reflections omitted from the refinement process.
[g] The Ramachandran plots were calculated using Procheck.[57]

Table 4. Molecular dockings of *S*-enantiomers of target compounds in the GluA2 LBD in complex with (*S*)-**37**.[a]

Compound	XP-score (kcal/mol)	Strain (kJ/mol)
8	–9.2	2.8
9	–9.4	1.1
10	–9.1	0.0
27	–10.2	4.4
28	–10.2	14.2
29	–8.4	10.6
30	–0.6	n.d.
31	–9.3	4.7
32	–1.3	n.d.
33	–8.1	0.3
34	–4.7	n.d.
35	–4.2	n.d.
36	–8.8	0.6
37	–9.8	6.3
38	–8.8	5.8

[a]: XP-scores and strain were calculated as described in the experimental section. The strain was determined for the bi-aromatic system, without the amino acid moiety of the ligand. n.d.: not determined.

Associated content

Supporting Information. Results of elemental analyses reported for target compounds

Accession Codes. Coordinates and structure factors have been deposited in the Protein Data Bank; (*S*)-**37** complex: *PDB ID* 5CBR and (*R*)-**38** complex: *PDB ID* 5CBS.

Author information

Corresponding Author

*Phone: (+45) 35 33 64 12. E-mail: tnj@sund.ku.dk

X-ray crystallography: Phone: (+45) 35 33 62 07. E-mail: karla.frydenvang@sund.ku.dk

Author Contributions

[c]E.S. (medicinal chemistry) and K.F. (X-ray crystallography) contributed equally to the work presented in this paper and are joint first authors.

Notes: The authors declare no competing financial interest.

Acknowledgements

Heidi Peterson is thanked for help with expression and purification of GluA2 LBD. MAX-lab, Lund, Sweden and ESRF, Grenoble, France are thanked for providing beamtime. Financial support of this research by The Danish Council for Independent Research/Medical Sciences, the Alfred Benzon Foundation, GluTarget and Danscatt and The Polish Ministry of Science, Higher Education and National Science Centre (grant No.N N405 303936) and the National Science Centre Poland (2014/15/B/NZ7/00908) are gratefully acknowledged.

Abbreviations used

AMPA, (*RS*)-2-amino-3-(3-hydroxy-5-methylisoxazol-4-yl)propionic acid; (*S*)-ATPO, (*S*)-2-amino-3-[5-*tert*-butyl-3-(phosphonomethoxy)-isoxazol-4-yl]propionic acid; CNS, central nervous system; Glu, (*S*)-glutamate; GluR2-S1S2J, ligand binding domain of the GluA2 receptor subunit; iGluRs, ionotropic glutamate receptors; KA, kainate; LBD, ligand binding domain; NBQX, 6-nitro-7-sulfamoyl-benzo[*f*]quinoxaline-2,3-dione; NMDA, *N*-methyl-D-aspartic acid; NS1209, (*S*)-8-methyl-5-(4-(*N,N*-dimethylsulfamoyl)phenyl)-6,7,8,9,-tetrahydro-1*H*-pyrrolo[3,2-*h*]-isoquinoline-2,3-dione-3-*O*-(4-hydroxybutyrate-2-yl)oxime; TEVC, two electrode voltage clamp; V_h, TEVC holding potential; UBP310, (*S*)-1-(2-amino-2-carboxyethyl)-3-(2-carboxy-thiophene-3-yl-methyl)-5-methylpyrimidine-2,4-dione; ZK-200775, 3,4-dihydro-7-(4-morpholinyl)-2,3-dioxo-6-trifluoromethyl-(2*H*)-quinoxalin-1-yl-methylphosphonic acid.

References

1. Traynelis, S. F.; Wollmuth, L. P.; McBain, C. J.; Menniti, F. S.; Vance, K. M.; Ogden, K. K.; Hansen, K. B.; Yuan, H.; Myers, S. J.; Dingledine, R. Glutamate receptor ion channels: structure, regulation, and function. *Pharmacol. Rev.* **2010,** 62, 405-96.
2. Stawski, P.; Janovjak, H.; Trauner, D. Pharmacology of ionotropic glutamate receptors: A structural perspective. *Bioorg. Med. Chem.* **2010,** 18, 7759-72.
3. Lemoine, D.; Jiang, R.; Taly, A.; Chataigneau, T.; Specht, A.; Grutter, T. Ligand-gated ion channels: new insights into neurological disorders and ligand recognition. *Chem. Rev.* **2012,** 112, 6285-318.
4. Chang, P. K.; Verbich, D.; McKinney, R. A. AMPA receptors as drug targets in neurological disease - advantages, caveats, and future outlook. *Eur. J. Neurosci.* **2012,** 35, 1908-16.
5. Catarzi, D.; Colotta, V.; Varano, F. Competitive AMPA receptor antagonists. *Med. Res. Rev.* **2007,** 27, 239-78.
6. Fleming, J. J.; England, P. M. Developing a complete pharmacology for AMPA receptors: a perspective on subtype-selective ligands. *Bioorg. Med. Chem.* **2010,** 18, 1381-7.
7. Larsen, A. M.; Bunch, L. Medicinal chemistry of competitive kainate receptor antagonists. *ACS Chem. Neurosci.* **2011,** 2, 60-74.
8. Møller, E. H.; Egebjerg, J.; Brehm, L.; Stensbøl, T. B.; Johansen, T. N.; Madsen, U.; Krogsgaard-Larsen, P. Resolution, absolute stereochemistry, and enantiopharmacology of the GluR1-4 and GluR5 antagonist 2-amino-3-[5-tert-butyl-3-(phosphonomethoxy)-4-isoxazolyl]propionic acid. *Chirality* **1999,** 11, 752-9.
9. Hogner, A.; Greenwood, J. R.; Liljefors, T.; Lunn, M. L.; Egebjerg, J.; Larsen, I. K.; Gouaux, E.; Kastrup, J. S. Competitive antagonism of AMPA receptors by ligands of different classes: crystal structure of ATPO bound to the GluR2 ligand-binding core, in comparison with DNQX. *J. Med. Chem.* **2003,** 46, 214-21.
10. Ahmed, A. H.; Thompson, M. D.; Fenwick, M. K.; Romero, B.; Loh, A. P.; Jane, D. E.; Sondermann, H.; Oswald, R. E. Mechanisms of antagonism of the GluR2 AMPA receptor: structure and dynamics of the complex of two willardiine antagonists with the glutamate binding domain. *Biochemistry* **2009,** 48, 3894-903.
11. O'Neill, M. J.; Bond, A.; Ornstein, P. L.; Ward, M. A.; Hicks, C. A.; Hoo, K.; Bleakman, D.; Lodge, D. Decahydroisoquinolines: novel competitive AMPA/kainate antagonists with neuroprotective effects in global cerebral ischaemia. *Neuropharmacology* **1998,** 37, 1211-22.
12. Wallace, M. S.; Lam, V.; Schettler, J. NGX426, an oral AMPA-kainate antagonist, is effective in human capsaicin-induced pain and hyperalgesia. *Pain Medicine* **2012,** 13, 1601-10.
13. Szymanska, E.; Frydenvang, K.; Contreras-Sanz, A.; Pickering, D. S.; Frola, E.; Serafimoska, Z.; Nielsen, B.; Kastrup, J. S.; Johansen, T. N. A new phenylalanine derivative acts as an antagonist at the AMPA receptor GluA2 and introduces partial domain closure: synthesis, resolution, pharmacology, and crystal structure. *J. Med. Chem.* **2011,** 54, 7289-98.
14. Venskutonyte, R.; Frydenvang, K.; Valades, E. A.; Szymanska, E.; Johansen, T. N.; Kastrup, J. S.; Pickering, D. S. Structural and pharmacological characterization of phenylalanine-based AMPA receptor antagonists at kainate receptors. *ChemMedChem* **2012,** 7, 1793-8.
15. Filliat, P.; Pernot-Marino, I.; Baubichon, D.; Lallement, G. Behavioral effects of NBQX, a competitive antagonist of the AMPA receptors. *Pharmacol. Biochem. Behav.* **1998,** 59, 1087-92.
16. Turski, L.; Huth, A.; Sheardown, M.; McDonald, F.; Neuhaus, R.; Schneider, H. H.; Dirnagl, U.; Wiegand, F.; Jacobsen, P.; Ottow, E. ZK200775: a phosphonate quinoxalinedione AMPA antagonist for neuroprotection in stroke and trauma. *Proc. Natl. Acad. Sci. U. S. A.* **1998,** 95, 10960-5.
17. Nielsen, E. Ø.; Varming, T.; Mathiesen, C.; Jensen, L. H.; Møller, A.; Gouliaev, A. H.; Watjen, F.; Drejer, J. SPD 502: a water-soluble and in vivo long-lasting AMPA antagonist with neuroprotective activity. *J. Pharmacol. Exp. Ther.* **1999,** 289, 1492-501.

18. Kasper, C.; Pickering, D. S.; Mirza, O.; Olsen, L.; Kristensen, A. S.; Greenwood, J. R.; Liljefors, T.; Schousboe, A.; Watjen, F.; Gajhede, M.; Sigurskjold, B. W.; Kastrup, J. S. The structure of a mixed GluR2 ligand-binding core dimer in complex with (S)-glutamate and the antagonist (S)-NS1209. *J. Mol. Biol.* **2006,** 357, 1184-201.
19. Armstrong, N.; Gouaux, E. Mechanisms for activation and antagonism of an AMPA-sensitive glutamate receptor: crystal structures of the GluR2 ligand binding core. *Neuron* **2000,** 28, 165-81.
20. Pøhlsgaard, J.; Frydenvang, K.; Madsen, U.; Kastrup, J. S. Lessons from more than 80 structures of the GluA2 ligand-binding domain in complex with agonists, antagonists and allosteric modulators. *Neuropharmacology* **2011,** 60, 135-50.
21. Sobolevsky, A. I.; Rosconi, M. P.; Gouaux, E. X-ray structure, symmetry and mechanism of an AMPA-subtype glutamate receptor. *Nature* **2009,** 462, 745-56.
22. Beich-Frandsen, M.; Pickering, D. S.; Mirza, O.; Johansen, T. N.; Greenwood, J.; Vestergaard, B.; Schousboe, A.; Gajhede, M.; Liljefors, T.; Kastrup, J. S. Structures of the ligand-binding core of iGluR2 in complex with the agonists (R)- and (S)-2-amino-3-(4-hydroxy-1,2,5-thiadiazol-3-yl)propionic acid explain their unusual equipotency. *J. Med. Chem.* **2008,** 51, 1459-63.
23. Ahmed, A. H.; Hamada, M.; Shinada, T.; Ohfune, Y.; Weerasinghe, L.; Garner, P. P.; Oswald, R. E. The structure of (-)-kaitocephalin bound to the ligand binding domain of the (S)-alpha-amino-3-hydroxy-5-methyl-4-isoxazolepropionic acid (AMPA)/glutamate receptor, GluA2. *J. Biol. Chem.* **2012,** 287, 41007-13.
24. Frydenvang, K.; Pickering, D. S.; Greenwood, J. R.; Krogsgaard-Larsen, N.; Brehm, L.; Nielsen, B.; Vogensen, S. B.; Hald, H.; Kastrup, J. S.; Krogsgaard-Larsen, P.; Clausen, R. P. Biostructural and pharmacological studies of bicyclic analogues of the 3-isoxazolol glutamate receptor agonist ibotenic acid. *J. Med. Chem.* **2010,** 53, 8354-61.
25. Juknaite, L.; Sugamata, Y.; Tokiwa, K.; Ishikawa, Y.; Takamizawa, S.; Eng, A.; Sakai, R.; Pickering, D. S.; Frydenvang, K.; Swanson, G. T.; Kastrup, J. S.; Oikawa, M. Studies on an (S)-2-amino-3-(3-hydroxy-5-methyl-4-isoxazolyl)propionic acid (AMPA) receptor antagonist IKM-159: asymmetric synthesis, neuroactivity, and structural characterization. *J. Med. Chem.* **2013,** 56, 2283-93.
26. Szymanska, E.; Pickering, D. S.; Nielsen, B.; Johansen, T. N. 3-Substituted phenylalanines as selective AMPA- and kainate receptor ligands. *Bioorg. Med. Chem.* **2009,** 17, 6390-401.
27. Armstrong, D. W.; Liu, Y.; Ekborg-Ott, K. H. A covalently bonded teicoplanin chiral stationary phase for HPLC enantioseparations. *Chirality* **1995,** 7, 474-97.
28. Berthod, A.; Liu, Y.; Bagwill, C.; Armstrong, D. W. Facile liquid chromatographic enantioresolution of native amino acids and peptides using a teicoplanin chiral stationary phase. *J. Chromatogr. A* **1996,** 731, 123-37.
29. Gübitz, G.; Jellenz, W.; Santi, W. Separation of the optical isomers of amino acids by ligand exchange chromatography using chemically bonded chiral phases. *J. Chromatogr.* **1981,** 203, 377-84.
30. Haynes, W. L. *CRC Handbook of Chemistry and Physics 96th Edition*. Taylor and Francis, Boca Raton, FL: 2015.
31. Hogner, A.; Kastrup, J. S.; Jin, R.; Liljefors, T.; Mayer, M. L.; Egebjerg, J.; Larsen, I. K.; Gouaux, E. Structural basis for AMPA receptor activation and ligand selectivity: crystal structures of five agonist complexes with the GluR2 ligand-binding core. *J. Mol. Biol.* **2002,** 322, 93-109.
32. Frandsen, A.; Pickering, D. S.; Vestergaard, B.; Kasper, C.; Nielsen, B. B.; Greenwood, J. R.; Campiani, G.; Fattorusso, C.; Gajhede, M.; Schousboe, A.; Kastrup, J. S. Tyr702 is an important determinant of agonist binding and domain closure of the ligand-binding core of GluR2. *Mol. Pharmacol.* **2005,** 67, 703-13.

33. Kaae, B. H.; Krogsgaard-Larsen, P.; Johansen, T. N. Synthesis of aryl- and heteroaryl-substituted 3-benzyloxyisothiazoles via Suzuki and Negishi cross-coupling reactions. *J. Org. Chem.* **2004,** 69, 1401-4.
34. Ransom, R. W.; Stec, N. L. Cooperative modulation of [3H]MK-801 binding to the N-methyl-D-aspartate receptor-ion channel complex by L-glutamate, glycine, and polyamines. *J. Neurochem.* **1988,** 51, 830-6.
35. Honore, T.; Nielsen, M. Complex structure of quisqualate-sensitive glutamate receptors in rat cortex. *Neurosci. Lett.* **1985,** 54, 27-32.
36. Braitman, D. J.; Coyle, J. T. Inhibition of [^{3}H]kainic acid receptor binding by divalent cations correlates with ion affinity for the calcium channel. *Neuropharmacology* **1987,** 26, 1247-51.
37. Sills, M. A.; Fagg, G.; Pozza, M.; Angst, C.; Brundish, D. E.; Hurt, S. D.; Wilusz, E. J.; Williams, M. [3H]CGP 39653: a new N-methyl-D-aspartate antagonist radioligand with low nanomolar affinity in rat brain. *Eur. J. Pharmacol.* **1991,** 192, 19-24.
38. Hermit, M. B.; Greenwood, J. R.; Nielsen, B.; Bunch, L.; Jørgensen, C. G.; Vestergaard, H. T.; Stensbøl, T. B.; Sanchez, C.; Krogsgaard-Larsen, P.; Madsen, U.; Bräuner-Osborne, H. Ibotenic acid and thioibotenic acid: a remarkable difference in activity at group III metabotropic glutamate receptors. *Eur. J. Pharmacol.* **2004,** 486, 241-50.
39. Madsen, U.; Pickering, D. S.; Nielsen, B.; Bräuner-Osborne, H. 4-Alkylated homoibotenic acid (HIBO) analogues: versatile pharmacological agents with diverse selectivity profiles towards metabotropic and ionotropic glutamate receptor subtypes. *Neuropharmacology* **2005,** 49 Suppl 1, 114-9.
40. Quirk, J. C.; Nisenbaum, E. S. Multiple molecular determinants for allosteric modulation of alternatively spliced AMPA receptors. *J. Neurosci.* **2003,** 23, 10953-62.
41. Greenwood, J. R.; Mewett, K. N.; Allan, R. D.; Martin, B. O.; Pickering, D. S. 3-hydroxypyridazine 1-oxides as carboxylate bioisosteres: a new series of subtype-selective AMPA receptor agonists. *Neuropharmacology* **2006,** 51, 52-9.
42. Ramanoudjame, G.; Du, M.; Mankiewicz, K. A.; Jayaraman, V. Allosteric mechanism in AMPA receptors: a FRET-based investigation of conformational changes. *Proc. Natl. Acad. Sci. U. S. A.* **2006,** 103, 10473-8.
43. Juknaite, L.; Venskutonyte, R.; Assaf, Z.; Faure, S.; Gefflaut, T.; Aitken, D. J.; Nielsen, B.; Gajhede, M.; Kastrup, J. S.; Bunch, L.; Frydenvang, K.; Pickering, D. S. Pharmacological and structural characterization of conformationally restricted (S)-glutamate analogues at ionotropic glutamate receptors. *J. Struct. Biol.* **2012,** 180, 39-46.
44. Winn, M. D.; Ballard, C. C.; Cowtan, K. D.; Dodson, E. J.; Emsley, P.; Evans, P. R.; Keegan, R. M.; Krissinel, E. B.; Leslie, A. G.; McCoy, A.; McNicholas, S. J.; Murshudov, G. N.; Pannu, N. S.; Potterton, E. A.; Powell, H. R.; Read, R. J.; Vagin, A.; Wilson, K. S. Overview of the CCP4 suite and current developments. *Acta Crystallogr., Sect. D: Biol. Crystallogr.* **2011,** 67, 235-42.
45. Kabsch, W. Xds. *Acta Crystallogr., Sect. D: Biol. Crystallogr.* **2010,** 66, 125-32.
46. McCoy, A. J.; Grosse-Kunstleve, R. W.; Adams, P. D.; Winn, M. D.; Storoni, L. C.; Read, R. J. Phaser crystallographic software. *J. Appl. Crystallogr.* **2007,** 40, 658-74.
47. Emsley, P.; Lohkamp, B.; Scott, W. G.; Cowtan, K. Features and development of Coot. *Acta Crystallogr., Sect. D: Biol. Crystallogr.* **2010,** 66, 486-501.
48. *Maestro version 9.1, Schrödinger, LLC, New York, NY, 2010*.
49. Moriarty, N. W.; Grosse-Kunstleve, R. W.; Adams, P. D. electronic Ligand Builder and Optimization Workbench (eLBOW): a tool for ligand coordinate and restraint generation. *Acta Crystallogr., Sect. D: Biol. Crystallogr.* **2009,** 65, 1074-80.
50. *MacroModel 9.8, Schrödinger, LLC, New York, NY, 2011*.
51. Adams, P. D.; Afonine, P. V.; Bunkoczi, G.; Chen, V. B.; Davis, I. W.; Echols, N.; Headd, J. J.; Hung, L. W.; Kapral, G. J.; Grosse-Kunstleve, R. W.; McCoy, A. J.; Moriarty, N. W.; Oeffner, R.; Read, R. J.; Richardson, D. C.; Richardson, J. S.; Terwilliger, T. C.; Zwart, P. H. PHENIX: a

comprehensive Python-based system for macromolecular structure solution. *Acta Crystallogr., Sect. D: Biol. Crystallogr.* **2010,** 66, 213-21.
52. Hayward, S.; Lee, R. A. Improvements in the analysis of domain motions in proteins from conformational change: DynDom version 1.50. *J. Mol. Graphics Modell.* **2002,** 21, 181-3.
53. *The PyMOL Molecular Graphics System, version 1.5.0.5, Schrödinger, LLC*.
54. Friesner, R. A.; Banks, J. L.; Murphy, R. B.; Halgren, T. A.; Klicic, J. J.; Mainz, D. T.; Repasky, M. P.; Knoll, E. H.; Shelley, M.; Perry, J. K.; Shaw, D. E.; Francis, P.; Shenkin, P. S. Glide: a new approach for rapid, accurate docking and scoring. 1. Method and assessment of docking accuracy. *J. Med. Chem.* **2004,** 47, 1739-49.
55. Halgren, T. A.; Murphy, R. B.; Friesner, R. A.; Beard, H. S.; Frye, L. L.; Pollard, W. T.; Banks, J. L. Glide: a new approach for rapid, accurate docking and scoring. 2. Enrichment factors in database screening. *J. Med. Chem.* **2004,** 47, 1750-9.
56. Friesner, R. A.; Murphy, R. B.; Repasky, M. P.; Frye, L. L.; Greenwood, J. R.; Halgren, T. A.; Sanschagrin, P. C.; Mainz, D. T. Extra precision glide: docking and scoring incorporating a model of hydrophobic enclosure for protein-ligand complexes. *J. Med. Chem.* **2006,** 49, 6177-96.
57. Laskowski, R. A.; MacArthur, M. W.; Moss, D. S.; Thornton, J. M. PROCHECK: a program to check the stereochemical quality of protein structures. *J. Appl. Crystallogr.* **1993,** 26, 283-91.

Table of Contents Graphics

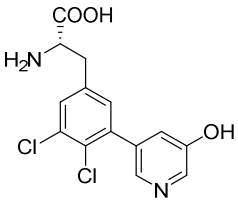

(*S*)-**37**

K_b = 1.80 μM

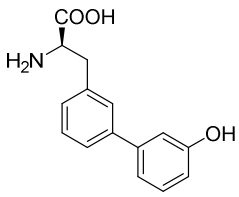

(*R*)-**38**

K_b = 3.90 μM

Homomeric GluA2 AMPA receptors